EFFECTS OF SURFACE MODIFICATION OF CARBON NANOTUBES (CNT) ON MECHANICAL & THERMAL PROPERTIES OF POLYPROPYLENE/CNT NANOCOMPOSITES

BY

SALIHU ADAMU GIREI

A Thesis Presented to the

DEANSHIP OF GRADUATE STUDIES

KING FAHD UNIVERSITY OF PETROLEUM & MINERALS

DHAHRAN, SAUDI ARABIA

In Partial Fulfillment of the
Requirements for the Degree of

MASTER OF SCIENCE

In

CHEMICAL ENGINEERING

JUNE 2010

KING FAHD UNIVERSITY OF PETROLEUM & MINERALS
DHAHRAN 31261, SAUDI ARABIA
DEANSHIP OF GRADUATE STUDIES

This thesis, written by Salihu Adamu Girei, under the direction of his thesis advisor and approved by his thesis committee, has been presented to and accepted by the Dean of Graduate Studies, in partial fulfillment of the requirements for the degree of

MASTER OF SCIENCE IN CHEMICAL ENGINEERING

Thesis Committee

Dr. Abdulhadi A. Al-Juhani
(Thesis Advisor)

Dr. Muataz Ali Atieh
(Co-Advisor)

Dr. Khaled Mezghani
(Member)

Dr. Adnan Al-Amer
(Departmental Chairman)

Dr. Abdulaziz A. As-Saadi
(Member)

Dr. Salam A. Zummo
(Dean of Graduate Studies)

25/2/10
Date

Dr. Sadhan Kumar De
(Member)

DEDICATION

This work is dedicated to my late step-mother Fadimatu Salihu Girei. May the almighty Allah (SWA) forgive her soul and accept her transition.

ACKNOLWLEDGEMENT

All praise is due to Allah (SWT) the lord of the worlds. May the peace and blessings of Allah be upon the Holy Prophet Mohammad (SAW) the leader of the mankind.

First and foremost, I thank Allah SWT for sparing my life and guiding me all through, to this very moment in my career. I thanked Him (Allah) for His divine guidance and the uncountable favours which He bestowed on me.

My profound gratitude goes to my thesis advisor, Dr. Abdulhadi A. Aljuhani who despite his schedules has found time for correction and reshaping of this work. I am moreover highly indebted to my co-advisor, Dr. Muataz Ali Atieh for his invaluable support, suggestion and contributions. To my thesis committee members: Dr. Khaled Mezghani, Dr. Abdulaziz As-Saadi and Chair Prof. Sadhan Kumar De, I thank you all for taking the pains to read through the original manuscript and for making useful suggestions. Without your countless effort, this work would not have gotten to this level.

My appreciation also extended to the Departmental Chairman, Faculty members, Staff and Graduate students of chemical engineering department. I also appreciate the company of Dr. Selvin Thomas, Dr. Sareekumar and Dr. Bijel, the three Post Doc fellows in my Department.

Special thanks go to my parents; Alhaji Adamu Girei & Hajja Fadimatu Imam for their religious and moral guidance. My uncles; Prof Mustapha Abba and Alhaji

Ahmad Imam, Elder Brothers; Mohammad Jika, Alhaji Idris, Alhaji Ma’azu Raji & Alhaji Bello Duzu. I thank you all for your support and encouragement.

Finally, my acknowledgment goes to this outstanding university in the Middle East, King Fahd University of Petroleum & Minerals (KFUPM) for proving me with scholarship and learning atmosphere and King Abdulaziz City of Science & Technology (KAUST) for funding this research work.

TABLE OF CONTENTS

LIST OF TABLES

LIST OF FIGURES

THESIS ABSTRACT

Full Name: Salihu Adamu Girei

Thesis Title: Effects of Surface Modification of Carbon Nanotubes (CNT) of the Mechanical and Thermal Properties of Polypropylene/CNT Nanocomposites

Major Field: Chemical Engineering

Date of Degree: June, 2010

In this work, Multiwall carbon nanotubes (MWCNTs) were functionalized with carboxylic (-COOH), Phenol (-phenolic), Octadecanol (C_{18}) and Dodecyamie (-amine) groups and characterized by using Fourier Transform Infrared Spectroscopy (FTIR). The composites of isotactic polypropylene (iPP) and MWCNT (iPP/MWCNT) was prepared in the melt state using co-rotating twin screw mini extruder. Scanning Electron Microscopy (SEM) images of the nanocomposites composites containing 1.0 wt.% CNTs loading indicates uniformed fractured morphology of nanotubes modified by phenolic group followed by nanotubes modified with Carboxylic. On the other hand, C_{18} and amine modification shows clusters and fiber like chunked fractured surface owing to aggregate formation and poor dispersion. The tensile properties of these composite were observed to increase with nanotubes loadings (0.1, 0.25, 1.00 and 5.00 wt. %) with a highest Young Modulus and tensile stress at 1.0 wt.% nanotubes loading. Moreover, in similitude with the SEM images, phenol modified MWCNTs gave better mechanical properties followed by MWCNT-COOH and MWCNT-C18. Nanotubes modified with amine

gave the least of enhancement in mechanical properties. The DSC analysis shows the nucleating effect of all the CNTs on the iPP matrix except for MWCNT-amine which shows no shift in DSC thermogram was observed at various nanotubes loadings. Overall degree of crystallinity changes with addition of MWCNT-COOH and MWCNT-Phenol whereas no changes in the degree of crystallinity were observed from MWCNT-C18 and MWCNT-amine.

.

جريد

الإسم: صالح آدم غيرى

عنوان الرساله: تأثير التعديلات السطحية لأنابيب الكربون متناهية الصغر (CNT) على الخصائص الميكانيكية والحرارية لخليط البولي بروبالين/ CNT.

الدرجة : ماجستير

التخصص: الهندسة الكيميائية

التاريخ : يونيو 2010

في هذه الدراسة, تم تعديل أنابيب الكربون متناهية الصغر بواسطه مجموعات الكربوكسيل, الفينول, الاوكتاديكانول والدوديسايل أمين وتم تشخيصها بواسطه جهاز (FTIR). تم تحضير خليط البروبالين وأنابيب الكربون متناهية الصغر في حالة الإنصهار بواسطة الاسطوانه الثنائية الدوارة. تم إستخدام جهاز الماسح الإلكتروني (SEM) لتصوير خلائط تحتوي على 0,1 %. وقد أظهرت النتائج توزيع جيد لأنابيب الكربون المعدلة بواسطه مجموعه الفينول ثم الكاربوكسيل.و من جهة أخرى؛ فان مجموعات الأمين والاوكتاديكانول أظهرت كتل عنقودية و الياف ذات اسطح مشققة و ذلك بسبب التكون التجميعي وضعف التشتت. تم ملاحظة أن خصائص التمدد تزداد من زيادة التحميل (0,1 % , 0,25% , 1% , 5 %) وأقصى معامل تمدد كان عند إستعمال 1% من أنابيب الكربون. من ناحية أخرى, أعطت العينات المضاف إليها الفينول خصائص ميكانيكية أفضل تليها مجموعة الكربوكسيل ثم الأمين . تمت دراسة التأثيرات النووية بواسطة جهاز DSC وتمت ملاحظة أن المخطط الحراري يتغير بتغير نسبة التحميل وكذلك درجة التبلور؛اما درجة التبلور لم تتغير عند إستخدام مجموعات الأمين والاوكتاديكانول .

CHAPTER 1

1 INTRODUCTION

1.1 BACKGROUND

Research on new materials and processing route provide opportunities for the production of advanced high performance structure for different applications. Polypropylene/Carbon Nanotubes (CNT) composites are one of these promising materials (Zdenko *et al.*, 2010). Carbon Nanotubes are graphitic sheets rolled into seamless tubes (i.e., arrangements of carbon hexagons into tube-like fullerenes) and have diameters ranging from about 1 to 100 nanometer (nm). Nanotubes have received much attention in composite formation and in there used as fillers (Iijima, 1999; Ebbesen *et al.*, 1996) in polymer matrices because of their outstanding properties (see Table: 1) since their discoveries in 1991 by Ijima.

The first ever polymer nanocomposites using CNTs as fillers were reported in 1994, by Ajayan *et al.*, since then, there have been many publications dedicated to processing and resulting mechanical and/or electrical properties of fabricated polymer nanocomposites. However, as-grown CNTs are normally mixtures of chiralities, diameters, and lengths, not to mention the presence of impurities and other defects.

Table 1: Properties of Carbon Nanotubes (CNT) (Yamabe 1995)

PROPERTIES OF CARBON NANOTUBES
Dimensions: 1nm (dia.) 0.3 - 100 µm (length
Density: 0.89g/cm3
Tensile Strength ~ 50 GPa
Tensile Modulus ~ 1TPa
Elongation to Failure ~ 5%
Electrical Conductivity ~1800-2000 ohms-1
Semiconducting to conducting like copper
Thermal conductivity (C_{60}) low in transverse direction and high (diamond) along tube axis (~2500 W/m•K)
Nanoscale scattering defects
- Tubes intact or removed in situ (nanovoids
Bonding by van der Waals or by functionalization

Furthermore, CNT aggregation has been found to dramatically hamper the mechanical properties of fabricated nanocomposites (Zdenko *et al.*, 2010). Finally, due to their small size, CNTs are normally curled twisted and therefore individual CNTs embedded in a polymer only exhibit a fraction of their potential. Thus, the outstanding properties of CNTs cannot as yet be fully translated into high strength and stiffness finished products.

Following these shortcomings, there has been an immense attempt to institute a most suitable condition for the transfer of either mechanical load or electrical charges to individual Nanotubes in polymer composite. A requirement for such endeavour is the efficient dispersion of individual Nanotubes and the establishment of strong chemical affinity with the surrounding polymer matrix. Researchers have used many different techniques to attempt to disperse nanotubes in polymer matrices, including solution chemistry to functionalize the nanotubes surface (Mitchell *et al.*, 2002; Bubert *et al.*, 2003 and Eitan *et al.*, 2003), use of polymers to coat the nanotubes surface (Star *et al.*, 2001), in situ polymerization of the nanocomposites (Star *et al.*, 2001; Deng *et al.*, 2002), ultrasonic dispersion in solution (Safadi *et al*., 2002; Qian *et al.*, 2000), melt processing (Potschke *et al.*, 2004; Siochi *et al.*, 2004, and Gorga *et al.*, 2004), use of surfactants (Shaffer *et al.*, 1998; Gong *et al.*, 2000), electrospinning (Dror *et al.*, 2003), gelation/crystallization (Bin *et al.*, 2003), and electrode chemistry(Chen, *et al.*, 2000). Furthermore, research has shown improved mechanical properties via nanotube orientation by melt drawing after melt compounding in a poly(methyl methacrylate) (PMMA) matrix with low levels (1wt %) of multiwall carbon nanotubes (MWNT) (Gorga *et al.*, 2004).

Recent studies have shown that, Polypropylene (PP) has been a common matrix used for carbon nanotube composites. Both single-wall (Bhattacharyya *et al.*, 2003; Valentini *et al.*, 2003), and multiwall (Xia *et al*., 2004), nanotubes have been used to study crystallization behavior in PP and polymer morphology as well as mechanical properties. Results have been mixed, especially for mechanical properties, where one study

(Bhattacharyya *et al.*, 2003) showed no significant improvement in mechanical properties, and others have shown moderate improvements in tensile strength, but decreased toughness (Moore *et al.*, 2004).

1.2 STATEMENT OF THE PROBLEM

Despite the outstanding mechanical, electrical and thermal properties of CNTs and their increasing potential as fillers for large variety of polymers (Lin *et al.,* 2007; Du 2007 *et al.,* and Coleman *et al.,* 2006), CNTs tend to aggregate into bundles and hence they are difficult to be dispersed homogeneously in polymer matrices. Furthermore, the strong intermolecular van der Waals interactions among the nanotubes in addition to weak polymer CNTs interfacial adhesion prevents efficient load transfer from the polymer matrix to the CNTs. As a result of poor dispersion and inefficient load transfer, the mechanical properties of polymer/CNTs are not as good as anticipated. In view of this it became imperative to search for most suitable, efficient method of homogeneous dispersion of CNTs into polymer matrices. From the forgoing literatures surveyed, it follows that surface modification of CNTs with organic moieties or polymers proves promising in reducing the dispersion and load transfer problems associated with Polymer/CNT nanocomposites formation.

1.3 RESAERCH OBJECTIVE AND SIGNIFICANCE

The objective of this work is to study the effect of MWCNTs on the mechanical, thermal and the morphological properties of polypropylene-based Nanocomposite. The primary objective is to investigate the effect of functionalized Nanotubes and Nanotubes concentrations on the mechanical and thermal properties of the composite. Furthermore, characterization of the composite matrix morphology will be investigated in a qualitative manner to ascertain the structure –property relationship of this system. The objectives of this research are hence summarized as follows:

1. To functionalize MWCNTs with different surfactants (carboxylic group, phenol, amine and C_{18}) followed by surface characterization of the functionalized nanotubes by using Fourier infrared spectroscopy (FTIR).
2. To develop MWCNT/Polypropylene nanocomposites by using melt blending technique in a twin screw mini extruder.
3. To study the morphology, thermal transition and mechanical properties of the developed nanocomposites by using Scanning Electron Microscopy (SEM), Differential Scanning Calorimery (DSC) and Instron Tensile Machine respectively.

CHAPTER 2

2 LITERATURE REVIEW

2.1 BACKGROUND

Since discovered by Iijima in 1991 Carbon Nanotubes (CNTs) have attracted more and more application as fillers for large variety of polymers due to their outstanding mechanical (Ruoff and Lorents 1995), thermal and electrical properties (Wong and Sheehan 1997). Two main type of carbon Nanotubes have high structural perfection. Singled-walled Nanotubes (SWNT) consist of a single graphite sheet seamlessly wrapped into a cylindrical tube. Multi-walleded Nanotubes (MWNT) comprise an array of Nanotubes that are concentrically nested. The Young's Modulus of a SWNT is as high as 5 TPa, Young's Modulus of MWNT is as high as 1.8 TPa and bending strengths as high as 14.2 GPa (Treacy *et al.*, 1996). CNTs are able to withstand repeated bending bucking and twisting which result in building lightweight nanocomposites matrix. CNTs have been considered as attractive candidates for important composition hybrids for fabricating novel materials with desired properties.

2.2 POLYPROPYLENE/CNT NANOCOMPOSITES

Carbon nanotubes (CNT) have high aspect-ratio structures with very good elastic and mechanical properties, and very high thermal and mechanical stability. These structural and material characteristics of nanotubes point towards their possible use in making next generation of extremely lightweight with highly elastic and very strong composite materials (Andrews and Wisenberger, 2004).

The most important application of nanotubes based on their mechanical properties will be as reinforcements in composite materials. The issue of nanotube dispersion is critical to efficient reinforcement. The main problem is in creating a good interface between nanotubes and the polymer matrix and attaining good load transfer from the matrix to the nanotubes, during loading. The reason for this is essentially two-fold. First, nanotubes are atomically smooth and have nearly the same diameters and aspect ratios (length/diameter) as polymer chains (Zdenko *et al.*, 2010). Second, nanotubes are usually organized into aggregates, which behave differently in response to a load, as compared to individual nanotubes. To maximize the advantage of nanotubes as reinforcing structures in high strength composites, the aggregates needs to be broken up and dispersed or cross-linked to prevent slippage. In addition, the surfaces of nanotubes have to be chemically modified (functionalized) to achieve strong interfaces between the surrounding polymer chains.

Seo et al. (2005) studied the reinforcement of polypropylene (PP) matrix resins by the incorporation of Carbon nanotubes (CNTs) in different contents of 0, 1, 2, 3, and 5 wt.%. The volume resistivity was measured to discover the percolation threshold of the

composites. The crystallization kinetics, organizations, and microstructures of CNTs/PP composites were investigated with differential scanning calorimeter (DSC), X-ray diffraction (XRD), and scanning electron microscopy (SEM) analyses, respectively. The Raman spectroscopy was also performed to obtain information on the CNTs/PP interactions. As a result, the volume resistivity was decreased with increasing the CNT content that could be governed in a percolation-like power law with a relatively low percolation threshold. And the crystallization exothermic peak shifted to a higher temperature, and the overall crystallization time was reduced by the increment of CNT content. Also, the nucleating effect of CNTs affected the crystallization of PP, but was not linearly dependent on the CNT content that meant a saturation of the nucleant effect at low CNT content.

Manchado et al (2005). Obtained a uniform dispersion of single-walled carbon nanotubes (SWNTs) in isotactic polypropylene (iPP) prepared by melt processing technique. The results obtained from the differential scanning calorimetry curves indicate that the addition of low SWNT amounts (less than 1 wt%) led to an increase in the rate of polymer crystallization with no substantial changes in the crystalline structure, as confirmed by X-ray diffraction. The tensile mechanical properties showed that Young's modulus and tensile strength considerably increase in the presence of nanotubes, with a maximum for 0.75 wt%. The reinforcing effect of SWNTs was also confirmed by dynamic mechanical analysis where, by adding nanotubes, a noticeable increase in the storage modulus was detected.

Seo and Park (2004) studied the influence of carbon nanotube (CNT) contents on electrical and rheological properties of CNTs-reinforced polypropylene (PP) composite. The volume resistivity of the composites was decreased with increasing the CNT content and the electrical percolation threshold was formed between 1 and 2 wt% CNTs, which were caused by the formation of conductive chains in the composites. The viscosity of the composites was increased with the addition of CNTs, which was accompanied by an increase in elastic melt properties (G'). This could be explained by the higher aspect ratio of the CNTs. The composites containing more than 2 wt% CNTs exhibited non-Newtonian curves at low frequency.

Bhattacharyya et al (2003) investigated the crystallization behavior of melt-blended polypropylene (PP)/single wall carbon nanotubes (SWNT) composites using optical microscopy and differential scanning calorimetry. PP/SWNT fibers have been spun using typical polypropylene melt spinning conditions. The PP crystallite orientation and the SWNT alignment in the fibers have been studied using X-ray diffraction and polarized Raman spectroscopy, respectively. The study reveals that polypropylene containing 0.8 wt% SWNT exhibits faster crystallization rate as compared to pure polypropylene.

Valentini et al (2003) studied the morphology of polypropylene matrix composites reinforced with single-walled nanotubes (PP-SWNTs). The characterization was performed by differential scanning calorimetry and Raman spectroscopy in order to obtain information on the matrix–nanotube interaction, on the crystallization kinetics of PP, and on the macrostructure and organization of the nanotubes in the composite. The results confirm the expected nucleating effect of nanotubes on the crystallization of

polypropylene. This effect is not linearly dependent on the SWNTs content, showing a saturation of the nucleating effect at low nanotube concentrations. Raman spectroscopy is successfully applied to demonstrate that in the composite films, the crystallization kinetics is strongly affected by the distance between the nanotubes bundles as a consequence of a different intercalation of the polymer.

Kashiwagi et al (2004) studied the thermal and flammability properties of polypropylene/multi-walled carbon nanotubes, (PP/MWNT) nanocomposites in the range of MWNT content from 0.5 to 4 wt%. Dispersion of MWNTs in these nanocomposites was characterized by SEM and optical microscopy. Flammability properties were measured with a cone calorimeter in air and a gasification device in a nitrogen atmosphere. A significant reduction in the peak heat release rate was observed; the greatest reduction was obtained with a MWNT content of 1 wt%. The radiative ignition delay time of the nanocomposites having less than 2% by mass of MWNT was shorter than that of PP due to an increase in the radiation in-depth absorption coefficient by the addition of carbon nanotubes. The effects of residual iron particles and of defects in the MWNTs on the heat release rate of the nanocomposite were not significant. The flame retardant performance was achieved through the formation of a relatively uniform network-structured floccule layer covering the entire sample surface without any cracks or gaps. This layer re-emitted much of the incident radiation back into the gas phase from its hot surface and thus reduced the transmitted flux to the receding PP layers below it, slowing the PP pyrolysis rate. To gain insight into these phenomena, thermal conductivities of the nanocomposites were measured as a function of temperature. While

the thermal conductivity of the nanocomposites increases with an increase in MWNT content, this increase is not as dramatic as the increase in electrical conductivity.

Dondero and Gorga (2006) studied the mechanical properties and morphology of multiwall carbon nanotubes (MWNT)/polypropylene (PP) nanocomposites as a function of nanotubes orientation and concentration. Through melt mixing followed by melt drawing, using a twin screw mini-extruder with a specially designed winding apparatus, the dispersion and orientation of MWNTs was optimized in PP. Tensile tests showed a 32% increase in toughness for a 0.25 wt % MWNT in PP (over pure PP). Moreover, modulus increased by 138% with 0.25 wt % MWNTs. Transmission electron microscopy and scanning electron microscopy demonstrated qualitative nanotube dispersion and orientation. Wide angle X-ray diffraction was used to study crystal morphology and orientation by calculating the Herman's orientation factor for the composites as function of nanotubes loading and orientation. The addition of nanotubes to oriented samples causes the crystalline morphology to shift from α and mesophase to only α phase. Furthermore, the addition of nanotubes (without orientation) was found to cause isotropization of the PP crystal, and drawing was shown to improve crystal orientation through the orientation factor. In addition, differential scanning calorimetry qualitatively revealed little change in overall crystallinity. The authors concluded that melt mixing coupled with melt drawing has yielded MWNT/PP composites with a unique combination of strength and toughness suitable for advanced fiber applications, such as smart fibers and high-performance fabrics.

Leelapornpisit et al (2005) investigated the effect of different concentrations of single-walled carbon nanotubes (SWNTs) on the nonisothermal crystallization kinetics, morphology, and mechanical properties of polypropylene (PP) matrix composites obtained by melt compounding. The characterization was done by X-ray diffraction, differential scanning calorimetry, optical and scanning electron microscopy, and dynamic mechanical thermal analysis. Microscopy showed well-dispersed nanotube ropes together with small and large aggregates. The modulus was found to increase by about 75% at a level of 0.5 wt % nanotubes. The SWNTs displayed a clear nucleating effect on the PP crystallization, favoring the α crystalline form rather than the β form. The crystallization kinetics analysis showed a significant increase in activation energy on incorporating nanotubes.

Yang et al (2005) prepared Nanocomposites made of atactic polypropylene (aPP) and multiwall carbon nanotubes by melt blending at 80°C with a Barabender mixer. The morphology, thermal stability, and dynamic mechanical properties of the obtained composites were studied subsequently. SEM observations indicate that the nanotubes are well dispersed in the aPP matrix. Each nanotubes is covered by a layer of aPP molecules. Thermal stability of the aPP in nitrogen is found to be enhanced significantly by the addition of nanotubes. Peak temperature of the DTG curve for the nanocomposite with 5 wt % nanotube loading shows about 70°C higher than that of pure aPP. Dynamic mechanical properties of aPP are also influenced by nanotubes, as shown by the increase in the storage modulus as well as significantly broadened loss tanδ peak. These effects of

nanotubes on the thermal stability and mechanical properties of aPP are explained by the adsorption effect of the aPP molecules on the nanotube surfaces in this study.

2.3 MODIFICATION OF CARBON NANOTUBES WITH SURFACTANTS

Carbon nanotubes CNTs usually agglomerate due to Van der Waals force existing between the carbon-carbon bonds, these rendered them extremely difficult to disperse and align in a polymer matrix. Thus, a significant challenge in developing high performance polymer/CNTs composites is to introduce the individual CNTs in a polymer matrix in order to achieve better dispersion and alignment and strong interfacial interactions, to improve the load transfer across the CNT-polymer matrix interface. A number of recent studies on functionalization revealed the usefulness of sidewall surface functionalization CNTs as reinforcing fillers for polymers (Yang *et al.*, 2007; Blond *et al*., 2006, Coleman *et al*., 2007 and Goh *et al.*, 2008). The surface modified CNTs reduce the tendency of nanotubes to aggregate and hence the nanotubes can be dispersed more homogeneously in the polymer matrix. Load transfer from the polymer matrix to nanotubes becomes more efficient through the functional group attached onto the nanotubes. As a result, mechanical and thermal properties of modified nanocomposites are superior to composites containing pristine CNTs.

2.4 PREPARATION METHODS OF POLYMER/CNT NANOCOMPOSITES

As emphasized in the preceding section, the dispersion of CNTs in polymer matrices is a critical issue in the preparation of CNT/polymer composites. Better reinforcing effects of

CNTs in polymer composites will be achieved if they do not form aggregates and as such, they must be well dispersed in polymer matrices. Currently there are several methods used to improve the dispersion of CNTs in polymer matrices, such methods as solution mixing, melt blending and in-situ polymerization method.

2.4.1 Solution Mixing

In this approach, CNTs dispersed in a suitable solvent are mixed with polymers dissolved in solution. The CNT/polymer composites are then formed by precipitating or by evaporating the solvent. It is well known that it is very difficult to properly disperse pristine CNTs in a solvent by simple stirring therefore to achieved dispersion using this process, a high power ultrasonication process used in forming a dispersion of CNTs. Ultrasonic irradiation has been extensively used in dispersion, emulsifying, crushing, and activating the particles. By taking advantage of the multi-effects of ultrasound, the aggregates and entanglements of CNTs can be effectively broken down. For example, Li et al. 2005 used a simple solution–precipitation technique to improve the dispersion of CNTs in a polycarbonate solution by sonication process. Their study showed that the CNTs were uniformly dispersed in polycarbonate matrix. Moreover, the work of Safadi et al. 2002, shows uniform dispersion of MWNTs in PS using ultrasonication. Recently Cho and co-workers 2006, prepared PU/MWNTs composites with better dispersion of CNTs up to 20 wt% in PU. In their work, the necessary weight fractions of carboxylate MWNTs were first dispersed in DMF solution under sonication at room temperature for 1 h using a high power ultrasonic processor.

2.4.2 Melt Mixing

For solution mixing, the matrix polymer must be soluble in at least one solvent. This is problematic for many polymers. Melt mixing is a common and simple method, particularly useful for thermoplastic polymers. In melt processing, CNTs are mechanically dispersed into a polymer matrix using a high temperature and high shear force mixer or compounder (Andrews et al. 2002). Melt mixing approach is simple and compatible with current industrial practices. The shear forces help to break nanotubes aggregates or prevent their formation. Valentini et al. 2005 prepared iPP/MWNTs composites via a melt compounding method using Haake Reomix internal mixer. Their study showed homogeneous dispersion of MWNTs in the matrix polymer matrix and gives rise to significant enhancements in mechanical properties. In fact, mixing has been successfully applied for the preparation of different polypropylene/CNT nanocomposites (Manchado el al. 2005; Zhang and Zhang 2007). Some polymer/CNTs composites processed using Melt blending techniques include high density PE/CNT (Tang W and Santare MH 2003, polycarbonate/CNT (Bhattacharyya 2004), PMMA/CNT (Pramoda el al. 2001) etc. The disadvantage of this method is that the dispersion of CNTs in a polymer matrix is quite poor compared to the dispersion that may be achieved through solution mixing. In addition, the CNTs must be lower due to the high viscosities of the composites at higher loading of CNTs

2.4.3 In-Situ Polymerization

In this polymerization method, the CNTs are dispersed in monomer followed by polymerization. A higher percentage of CNTs may be easily dispersed in this method, and form a strong interaction with the polymer matrixes. This method is useful for the preparation of composites with polymers that cannot be processed by solution or melt mixing, e.g., insoluble and thermally unstable polymers. Hu et al. 2007 synthesized MWNT-reinforced polyimide nanocomposites by in-situ polymerization of monomers in the presence of acylated MWNTs. They functionalized MWNTs with acyl groups, and then reacted with 3,3`,4,4`-biphenyltetracarboxylic dianhydride to form MWNT-poly(amic acid). The final MWNT-polyimide nanocomposite films were obtained by imidization of MWNT-poly-(amic acid) at 350◦C for 1 h under vacu um. Their results uniform dispersion of CNTs in the polymer matrix. Recently, Cho et al. 2007 fabricated MWNTs-reinforced polyimide nanocomposites by in-situ polymerization using 4,4`-oxydianilline, MWNT-COOH, and pyromellitic dianhydride followed by casting, evaporation, and thermal imidization. A homogeneous dispersion of MWCNT-COOH was achieved in polyamide matrix as evidenced by scanning electron microscopy.

2.5 MECHANICAL PROPERTIES OF POLYPROPYLENE/CNT NANOCOMPOSITES

As earlier pointed out, the one dimensional structure of CNTs, their low density, their high aspect ratio and extraordinary mechanical properties makes them particularly attractive as reinforcements in composite materials. Table 1 represents some of the literature data on CNT/Polypropylene composites mechanical characteristics like tensile

Table 2: Mechanical properties of polypropylene/CNT nanocomposites

Matrix	CNT type	CNTweight Fraction (%)	Processing Method	Tensile strength (% incr.)	Y. modulus (% incr.)	Toughness (% incr.)	Storage Modulus (% incr.)	Mechanical testing	Reference number
PP	Pure SWCNT	1.00	SMMS	40	55			Tensile	22
PP	Purified SWCNT	1.80	Solution Mixing				15	DMA	16
PP	Purified MWCNTs	1.00	PMMM	20	15			Tensile	45
PP	Pristine SWCNTs	1.00	MFS	45			42	Tensile, DMA	28
PP	Pristine SWCNTs	1.00	SMFS	150	200			Tensile	7
PP	Pristine SWCNTs	0.75	Shear Mixing	15	40		60	Tensile, DMA	24
PP	Pristine SWCNTs	0.50	Melt Mixing				75	DMA	23
PP	Pristine MWCNTs	0.25	MFS	10	130	30		Tensile	11
PP	Fluorinate SWCNTs	10.00	SMS	150	110			Tensile	25
PP	Oxidized MWCNTs	0.60	DPIM	20	300			Tensile	47
P/PP-g-MA 0:10	**C_{18}-alkyl modified MWCNTs**	**0.30**	**DPIM**	**40**	**40**			**100**	**50**

(Abbreviation of all processing methods are given in page 81, appendix C)

strength at elastic modulus and toughness.

CHAPTER 3

3 EXPERIMENTAL SECTION

This section explained the step by step procedures applied in obtaining the results discussed in Chapter 4. It highlights the methods and procedures for surface modification of CNTs and the Fourier Infrared Spectroscopy FTIR characterization techniques. The later section discusses nanocomposites preparations and its characterization through the use of Scanning Electron Microscopy (SEM), Differential Scanning Calorimetry (DSC) and Instron Tensile Testing machine.

3.1 CHEMICAL MODIFICATION OF MULTIWALL CARBON NANOTUBES

In order to enhance the dispersion of CNTs in Polypropylene, commercially available pristine MWCNTs (produced by Nanostructured and Amorphous Materials Inc., USA, 8 - 15nm diameter, 10-50μm length, 95% 230m2/g) was functionalized with COOH followed by modification with different surfactants as highlighted.

3.1.1 Acid Modification of MWCNT

The CNTs were mixed with concentrated nitric acid at a ratio of 1:10 in a round bottom flask and refluxed for 48 hours at 130 °C under continues stirring to obtain CNT-COOH modified MWCNTs (Bae JH et al, 2007). Upon cooling, the mixture was thoroughly filtered, washed continuously with deionized water to remove the last traces of unreacted

acid until the pH value was 6 which signifies zero acidity. The acid modified multiwall carbon nanotubes, henceforth MWCNT-COOH was finally filtered and dried at 60 °C (Bae JH et al, 2007).

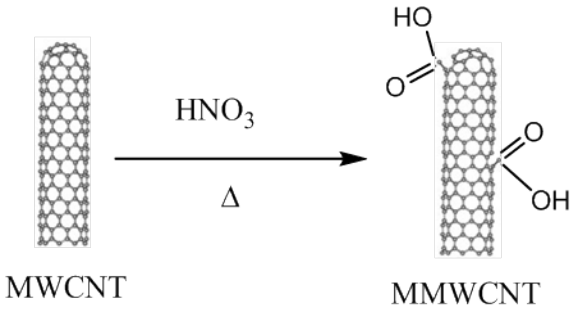

Figure 1: Mechanism of acid modification of carbon nanotubes (MWCNT) via thermal oxidation

3.1.2 Substitution of Carboxyllic (–OOH) Group with Different Surfactants

Surface functionalization of CNTs with surfactants was achieved by substitution of the MWCNT-COOH with appropriate surfactant such as 1-Octadecanol (C18), Phenol and Dodecyamine (Amine) at the surfactant melting temperature (Huges M., et al 2002). The first functionalization carried out was the substitution carboxylic group in MWCNT-COOH with 1-Octadecanol ($C_{18}H_{38}O$). For this purpose, 5g of MWCNT–COOH nanotubes was collected from the bulk samples of the acid modified CNTs and reacted with C_{18} in a few drops of sulfuric acid at a MWCNT-COOH to C_{18} ratio of ratio 1:10 and a temperature of 59.8°C for six (6) hrs under continuous stirring. The reaction takes place as shown in the scheme below

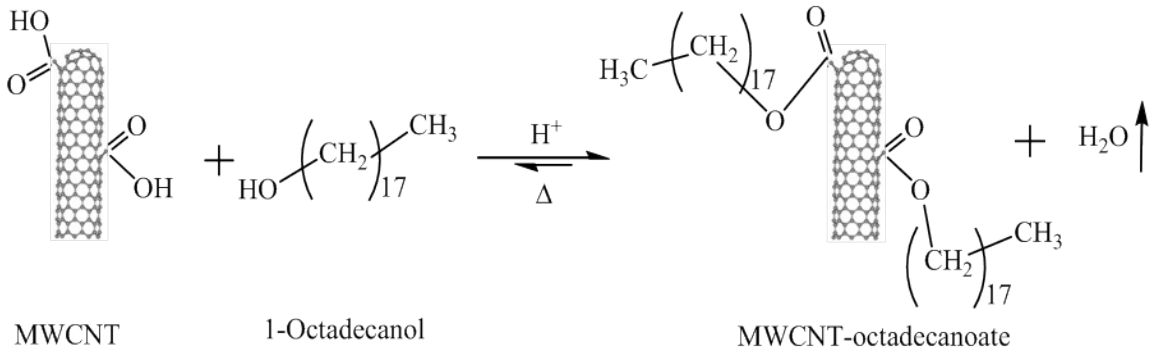

Figure 2: Mechanism of C_{18} modification of MWCNT (MWCNT-C_{18})

The resulting mixture was allowed to cool down, then washed and filtered in excess toluene solution and deionized water to remove traces of unreacted 1-Octadecanol and sulfuric acid respectively.

For functionalization with Amine group, Dodecylamine was used as a surfactant. In this case, 5g of MWCNT-COOH was added into a round bottom flask containing few drops of sulfuric acid. 50g of Dodecylamine was added and the mixture was heated with continues stirring at 30 °C for six (6) hrs. The content was allowed to cold, washed with Toluene and excess deionized water. The scheme was shown as follows.

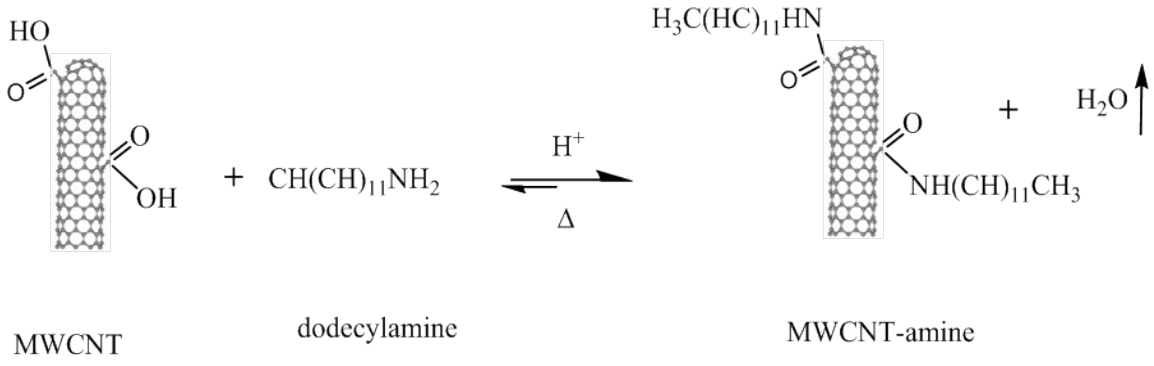

Figure 3: Mechanism of Amine modification of MWCNT (MWCNT-amine)

The last substitution of MWCNT-COOH with surfactants was for the phenol group. Here, phenol was mixed with MWCNT-COOH in a few drops of sulfuric acid at a ratio 10:1. The mixed was then heated at 42 °C with continuous stirring for about six (6) hrs to obtained phenol modified CNTs. The content was allows to cool as with the previous substitution processes, then washed with Toluene and excess deionized water to removed any unreacted phenol and sulfuric acid.

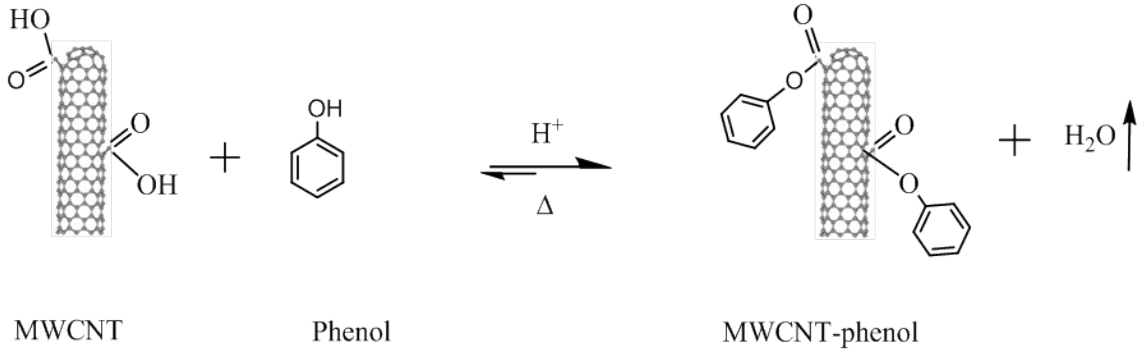

Figure 4: Mechanism of phenol modification of MWCNT (MWCNT-phenol)

3.2 NANOTUBES CHARACTERIZATION

Fourier transform infrared spectroscopy (FTIR) was used for the study of the surface chemistry of both the pure and modified carbon nanotubes. The spectra emitted by each surfactants i.e. -COOH, -C_{18}, -amine and -phenol was determine qualitatively within a range of 400 and 4000 cm^{-1} by using Nicolet 6700 FITR spectrometer from the Nicolet Instrument Corporation USA.

3.3 NANOCOMPOSITE PREPARATIONS

A commercially available isotactic Polypropylene (iPP) pellets (PP510P, SABIC Saudi Arabia) with density 905 kg/m^3 (ASTM D792 testing method) and MFR= 12 g/10 min (ASTM D 1238 testing method) was utilized as a matrix for this investigation. The pellets were grinded into powder to enhance their pre-mixability with CNTs. A control sample of a neat polypropylene was prepared from the iPP pellet prior to the nanocomposites preparations.

PP/CNTs nanocomposites were first and foremost prepared by pre-mixing of the powdered iPP with loadings (0.10, 0.25, 1.00, and 5.00 wt. %) of the pure and the functionalized nanotubes. Following this pre-mixing, the resulting composite was blended by using Haake twin screw mini extruder/mixer at 180 °C and speed of 100 rpm for 10 minutes. The blended samples were collected and compressed under a pressure of about 9 tons at 190 °C for 15 minutes by using Carver hydraulic hot-press. The same procedure was repeated for the CNTs with different modification.

3.4 NANOCOMPOSITE CHARACTERIZATION

In other to understand the effects of nanotubes dispersion into the polymer matrices, a morphological study of the nanotubes and iPP/CNTs nanocomposites samples was conducted by using scanning electron microscope (SEM) Model JOEL JSM-840A. Thermal transition of the composite was evaluated by using non-isothermal DSC analysis. The analysis was performed by using TA Q1000 instrument equipped with liquid nitrogen cooling system and auto sampler. A standard procedure in non isothermal scans were as follows: samples of about 8mg were heated in non-hermetic aluminum pans from 20 to 200 °C at a scan rate of 5 °C/min and held for 5 min to erase the thermal and mechanical history incurred during sample preparation. The samples were non-isothermally crystallized from 250 to -40°C at a cooling rate of 5 °C/min and subsequently, the melting point was measured by raising the temperature to 250°C at a similar rate. On the other hand, a tensile testing was conducted using an Instron machine Model 5567 at room temperature and a speed of 5 mm/min. The testing procedure adopted for these purpose was ASTM-D638. The average test specimen (dog bone) dimensions were 15 mm x 3.9 mm x 1 mm. A minimum of five samples were tested for each CNTs composition.

CHAPTER 4

4 RESULTS AND DISCUSSIONS

In this chapter, experimental results are presented and discussed. The experimental discussions on the results of the effects of functionalization of carbon nanotubes on mechanical and thermal properties of polypropylene were designed in four stages. The first section covers characterization of surface chemistry of the modified Carbon nanotubes using Fourier infrared spectroscopy (FTIR) and Scanning Electron Microscopy (SEM). While the remaining three stages involve discussion on the characterization of morphological, thermal and mechanical properties of polypropylene/CNT nanocomposites with the aid of Scanning Electron Microscopy (SEM), Differential Scanning Calorimetry (DSC) and Instron Tensile Testing Machine respectively. For simplicity, the effect of each of the surfactant used in this study was considered separately.

4.1 THE INFRARED SPECTROSCOPY CHARACTERIZATION (FTIR)

In order to identify the existence of functional groups on the MWCNTs surface, Fourier transform infrared spectroscopy (FTIR) was conducted for all the nanotubes in the range of 400 to 4000 cm^{-1}. FTIR spectroscopy has been widely employed in the determination of structure of molecules (Socrates G. 1980). Its application in the study of surface chemistry has provided one of the direct means of observing the interaction and

perturbations that occur at the surface during adsorption and in determining the structure of the absorbed species. Fig. 5 shows the spectra of unmodified MWCNT.

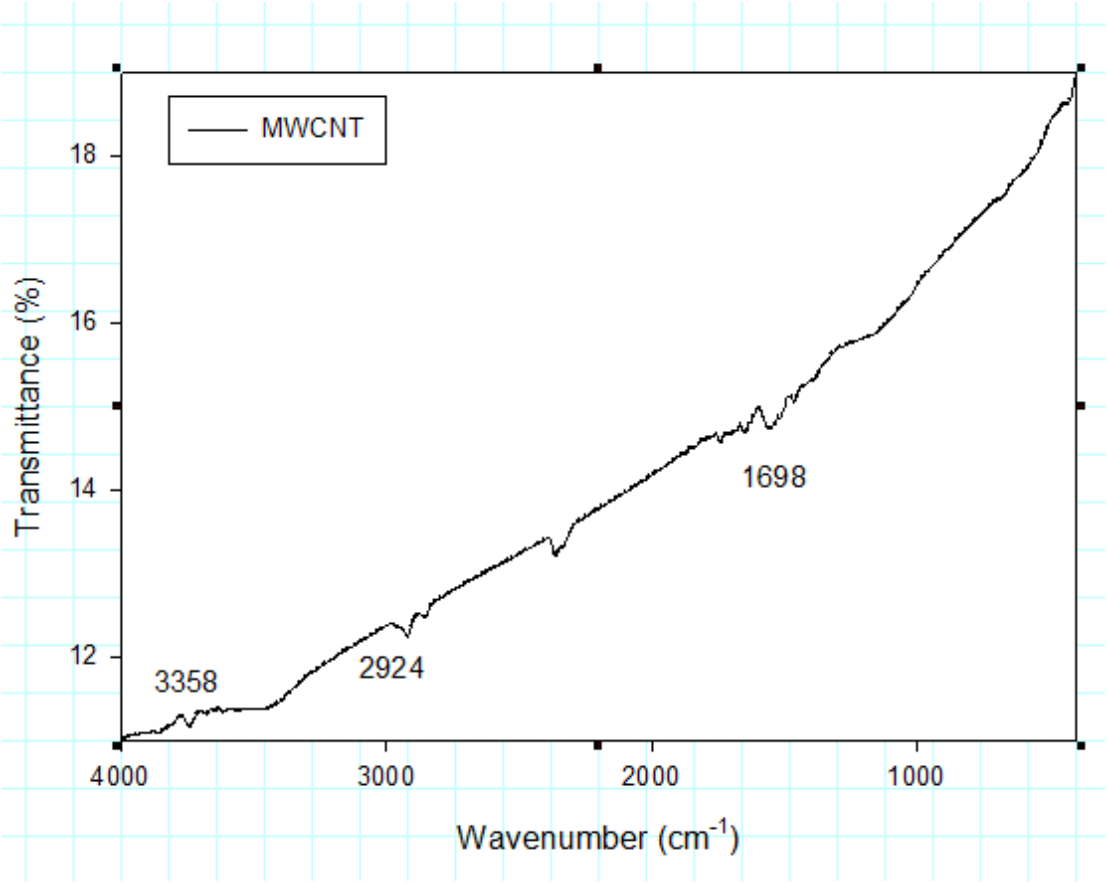

Figure 5: FTIR spectrum of unmodified multiwall carbon nanotubes (MWCNT)

The IR spectrum for the unmodified MWCNT shows absorption band at 3358 cm^{-1} attributed to hydrogen bonded O-H stretching, 2920 cm^{-1} which is attributed to symmetric and asymmetric CH_2 stretching and 1698 cm^{-1} (assigned to carboxylic C=O stretching for acids groups. The presence of these functional groups on the surface of pure MWCNTs indicates their introduction during removal of metal catalysts in

nanotubes purification processes. On acid modification of the nanotubes with concentrated nitric acid, a new spectrum was obtained as shown in the Figure 6 below

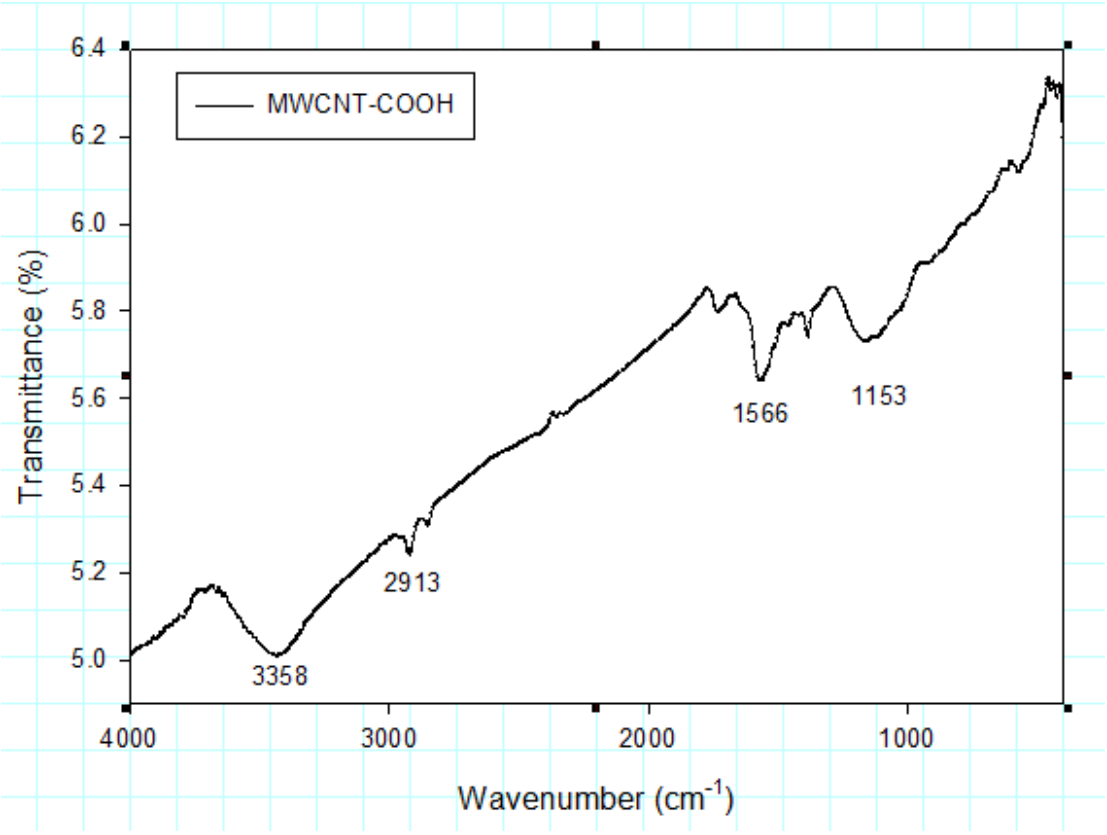

Figure 6: FTIR spectrum of acid modified multiwall carbon nanotubes (MWCNT-COOH)

In this new IR spectrum of MWCNT-COOH, an adsorption band at 3358 cm^{-1} (hydrogen bonded O-H stretch) is ascribed to the characteristic spectrum of carboxylic acid. As can be seen from figure Fig 6 above, this particular peak is usually broad and can obscure other peaks within the entire region of 3400 to 2400 cm^{-1}. Moreover, carboxylic peak C=O stretching peak is observed at 1693 cm^{-1}. The existence of these peaks signified the

success of surface modification of the CNTs with carboxylic acid group. Similarly, substitution of MWCNT-COOH with phenolic group (Figure 7) gives indicative peaks at 1452 cm^{-1} (corresponding to C-C=C asymmetric stretching for Aromatic rings) and a strong peak at 1228 cm^{-1} due C-O stretching of phenolic ester.

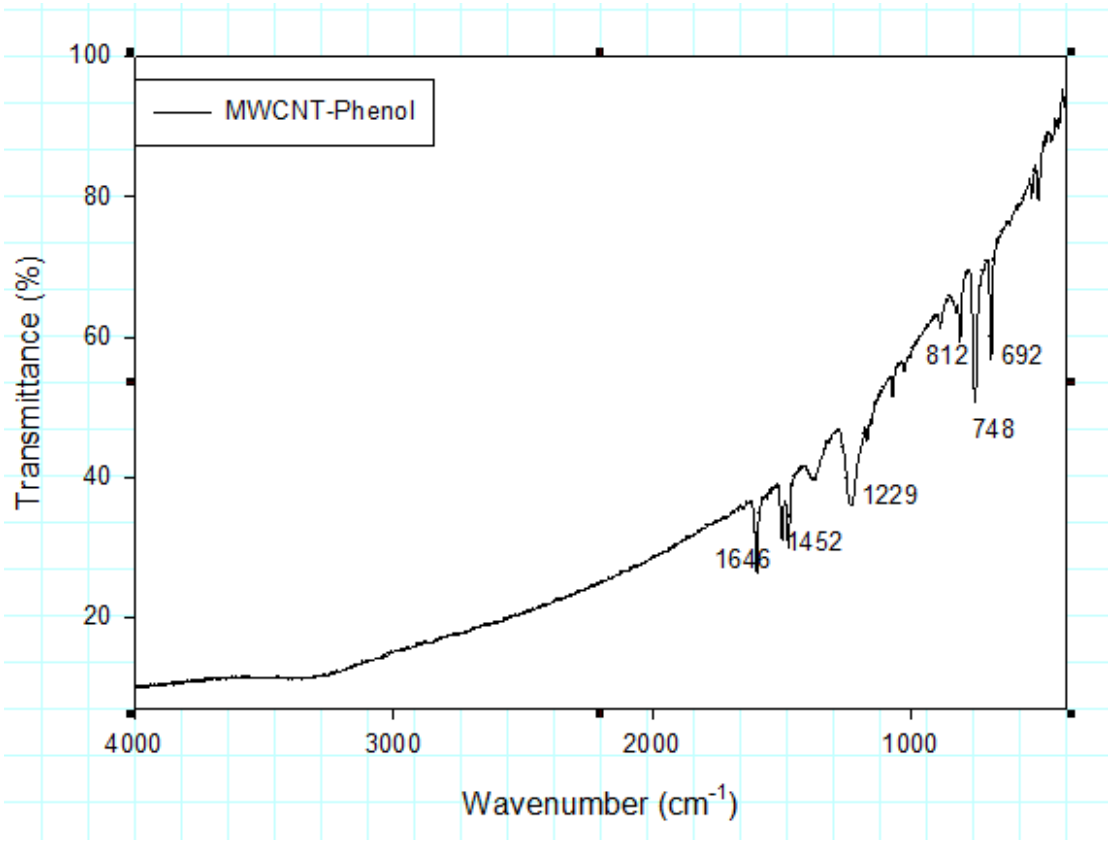

Figure 7: FTIR spectrum of phenol modified multiwall carbon nanotubes (MWCNT-Phenol)

Moreover, strong peaks at 812 cm^{-1}, 748 cm^{-1} and 692 cm^{-1} indicating the existence of phenoxide groups generated from the reaction between carboxylic COOH and phenyl alcohol was also indentified.

Figure 8 shows the IR spectrum modification of MWCNT-COOH with 1-Octadecanol.

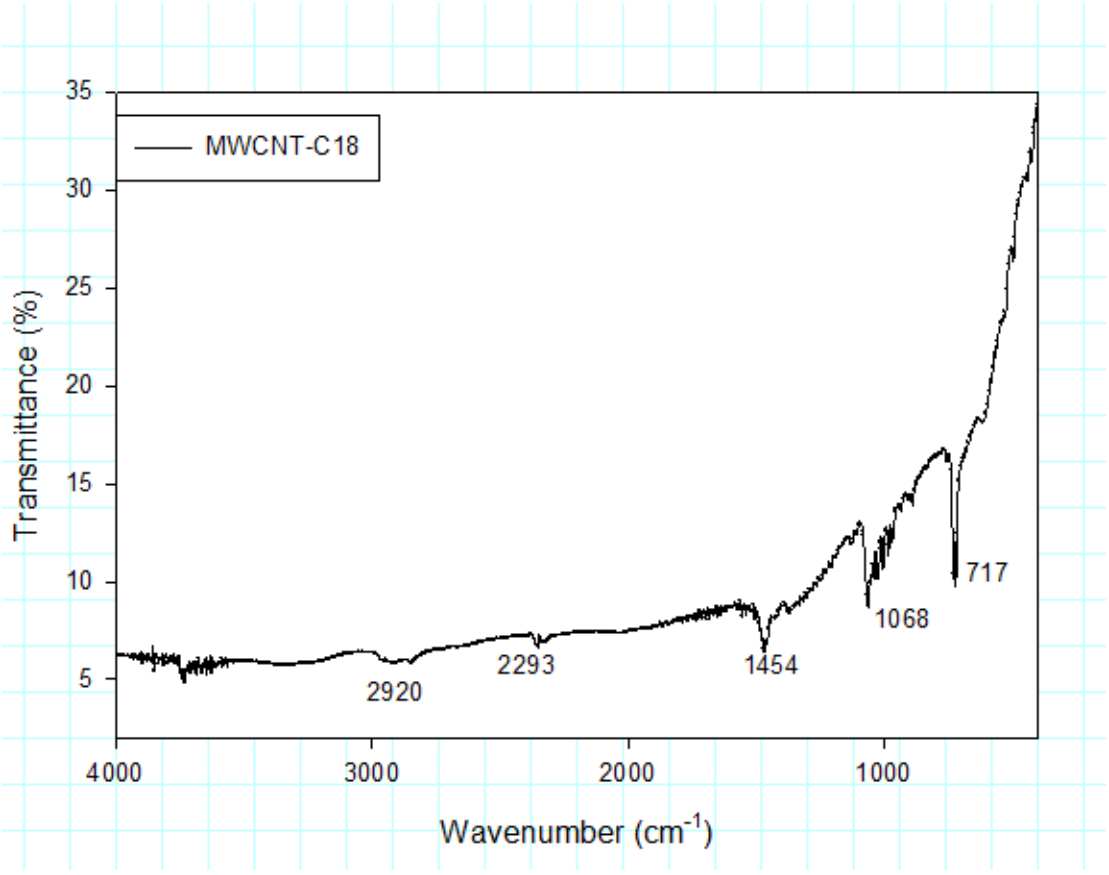

Figure 8: FTIR spectrum of C18 modified multiwall carbon nanotubes (MWCNT-C18)

An indicative peaks at 2920 cm^{-1} correspond to CH_2 stretching of long alkyl molecule of 1-Octadecanol emanates upon modification of MWCNT-COOH to MWCNT-C_{18}. In addition, modification with Octadecanol gives a medium C-H stretch and C-H bend of alkanes at 2293 cm^{-1} and 1454 cm^{-1} respectively. An indicative of long chain alkyl ester at 1068 cm^{-1} generated from esterification reaction of OH group of Octadecanol and COOH group of acid modified carbon nanotubes was also identified. Finally, a peak

showing C-H sharp bend at 717 cm^{-1} also indicate the success of MWNCT-COOH modification with Octadecanol. Thus we have MWCNT-C18 modified carbon nanotubes.

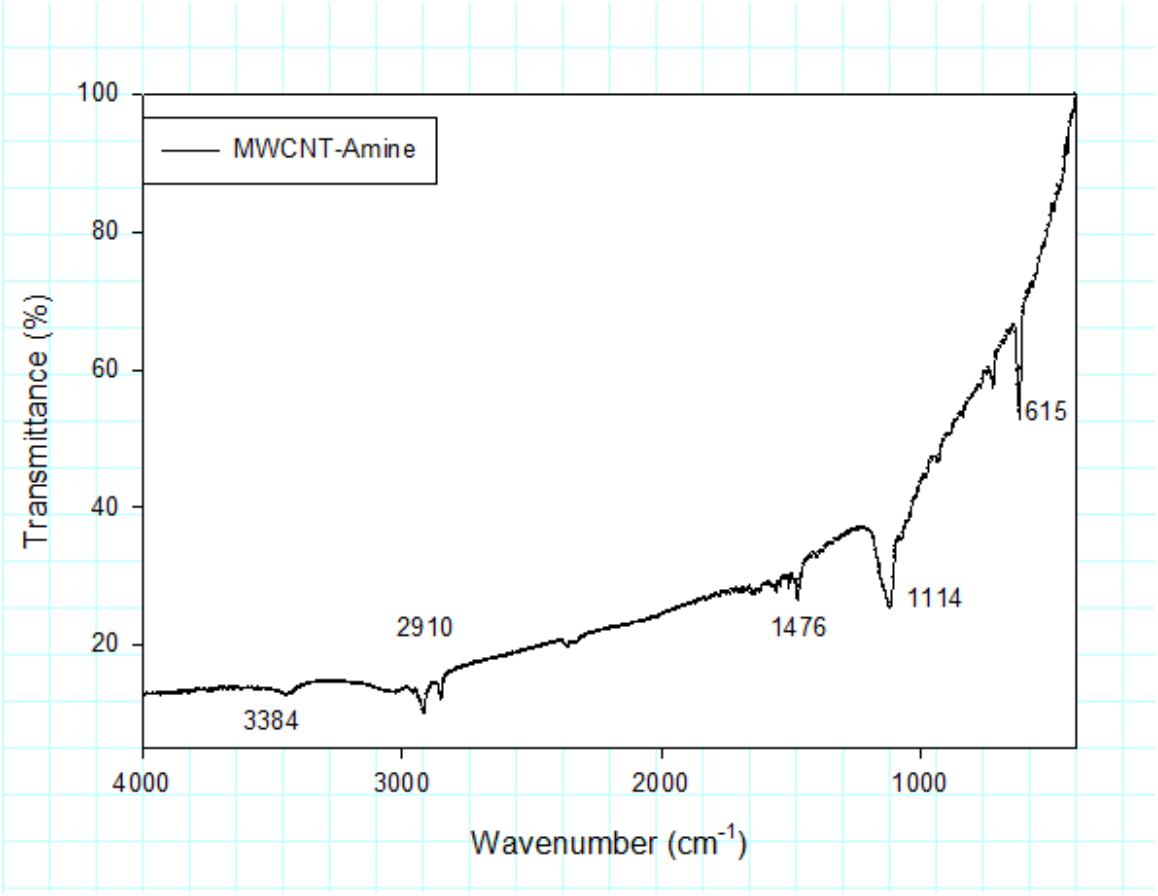

Figure 9: FTIR spectrum of amine modified multiwall carbon nanotubes (MWCNT-amine)

Nanotubes modification with Dodecylamine (Figure 9) gives a peak at 3384 cm^{-1} (N-H stretch for amides), 1476 cm^{-1} strong N-O asymmetric stretching for nitro compounds and 1114 cm^{-1} medium C-N stretch indicative peak for aliphatic amines. Lastly MWCNT-COOH modification with Dodecylamine gives N-H wag peak at 615 cm^{-1} for primary or secondary amine.

4.2 EFFECT OF PHENOL MODIFICATION ON THERMAL AND MECHANICAL PROPERTIES OF POLYPROPYLENE/CNT NANOCOMPOSITES

4.2.1 Nucleating behavior and thermal analysis of iPP/MWCNT-phenol nanocomposites

The effects of incorporating both modified and unmodified MWNTs on the crystallization of iPP at a cooling rate of $5^{o}C\ min^{-1}$ were investigated by non-isothermal DSC experiments. Fig. 10-12 shows DSC cooling and melting thermograms obtained for iPP/MWCNT, iPP/MWCNT-COOH and iPP/MWCNT-Phenol nanocomposites.

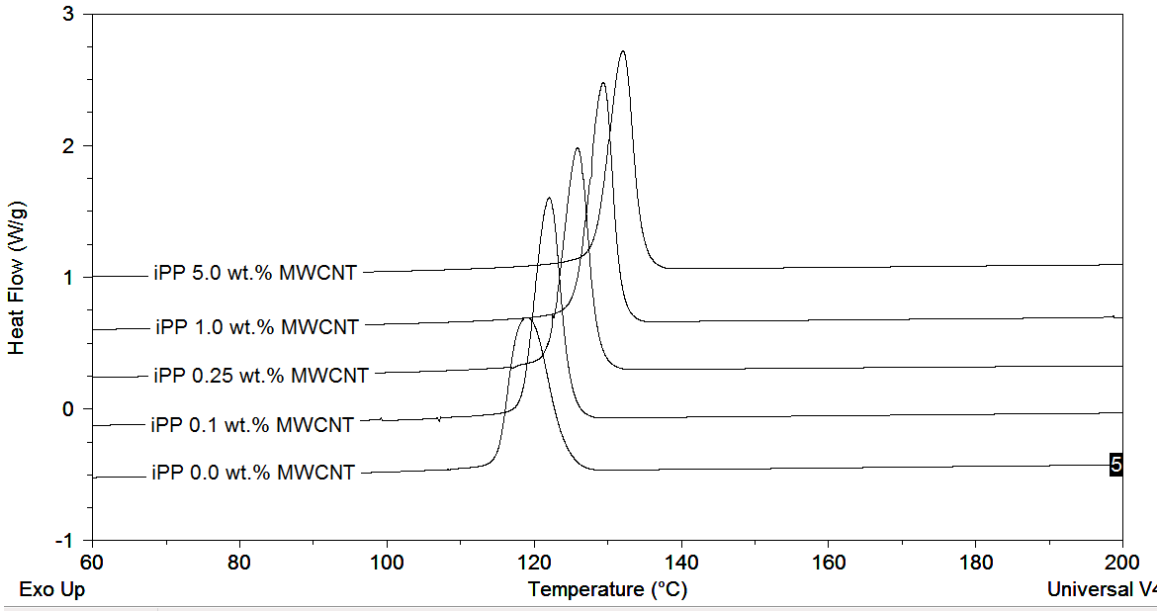

(a)

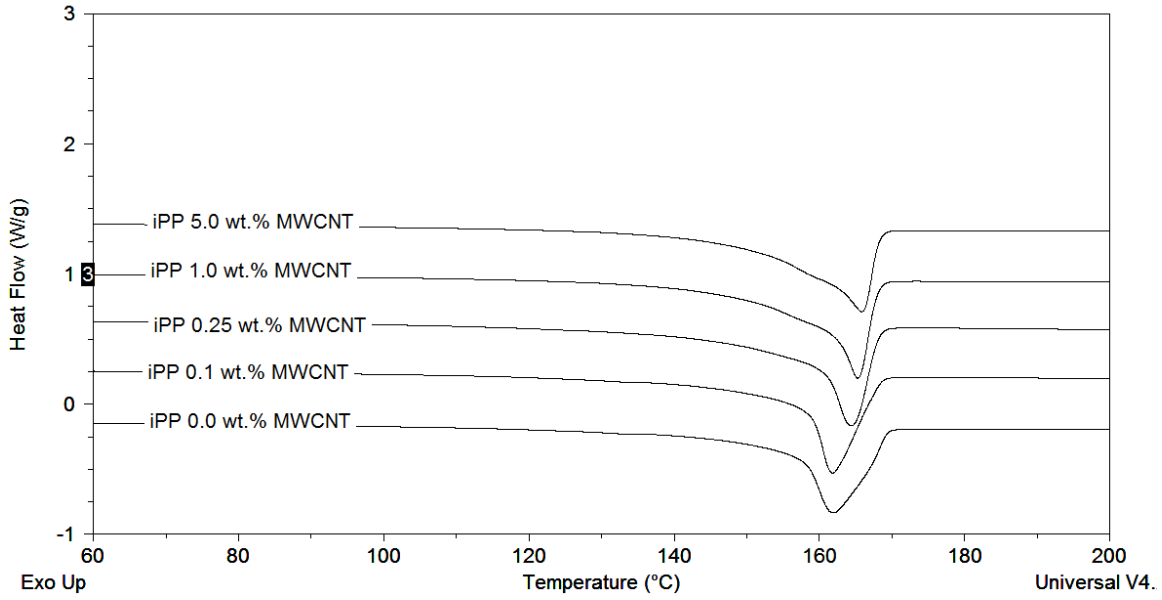

(b)

Figure 10: DSC thermograms of non-isothermal crystallization; (a) cooling peak of iPP/MWCNT, (b) Melting peaks of iPP/MWCNT

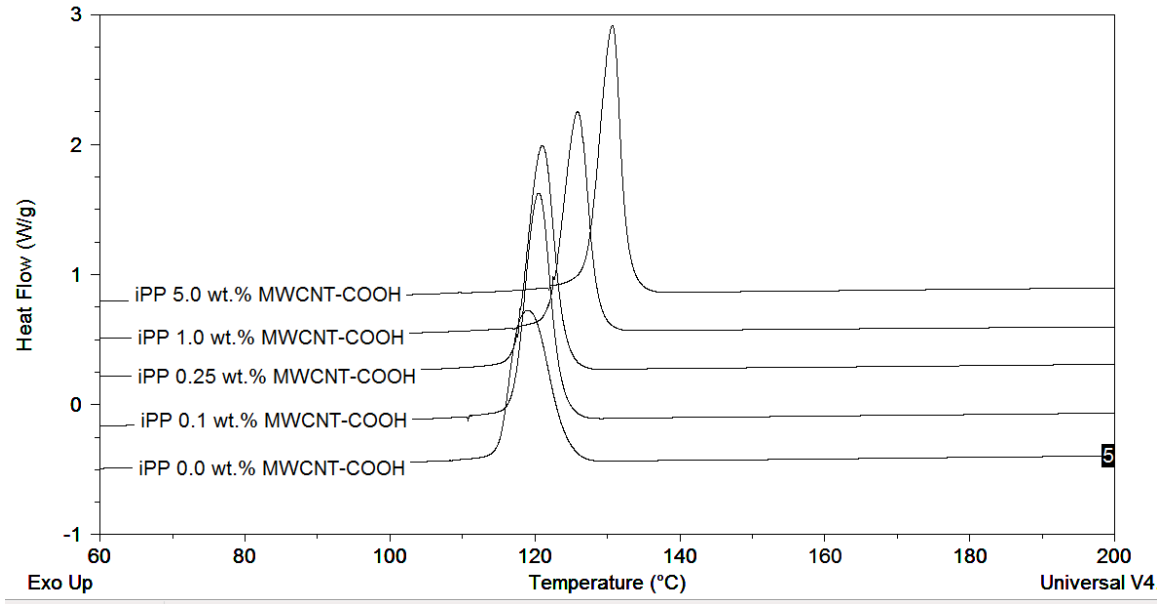

(c)

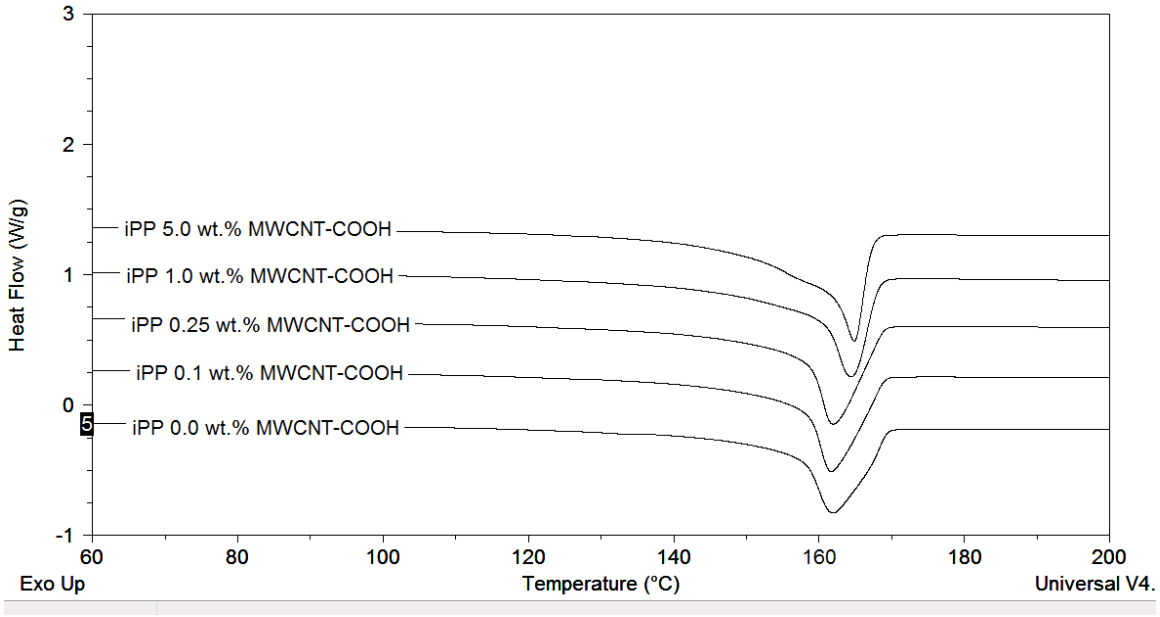

(d)

Figure 11: DSC thermograms of non-isothermal crystallization; (c) cooling peak of iPP/MWCNT, (d) Melting peaks of iPP/MWCNT-COOH

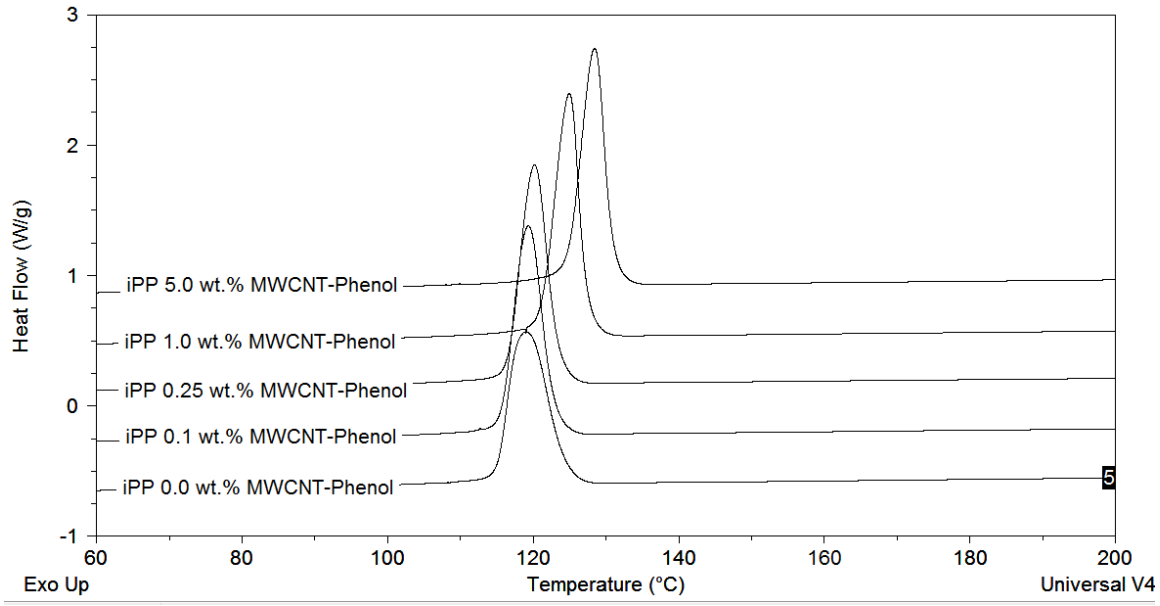

(e)

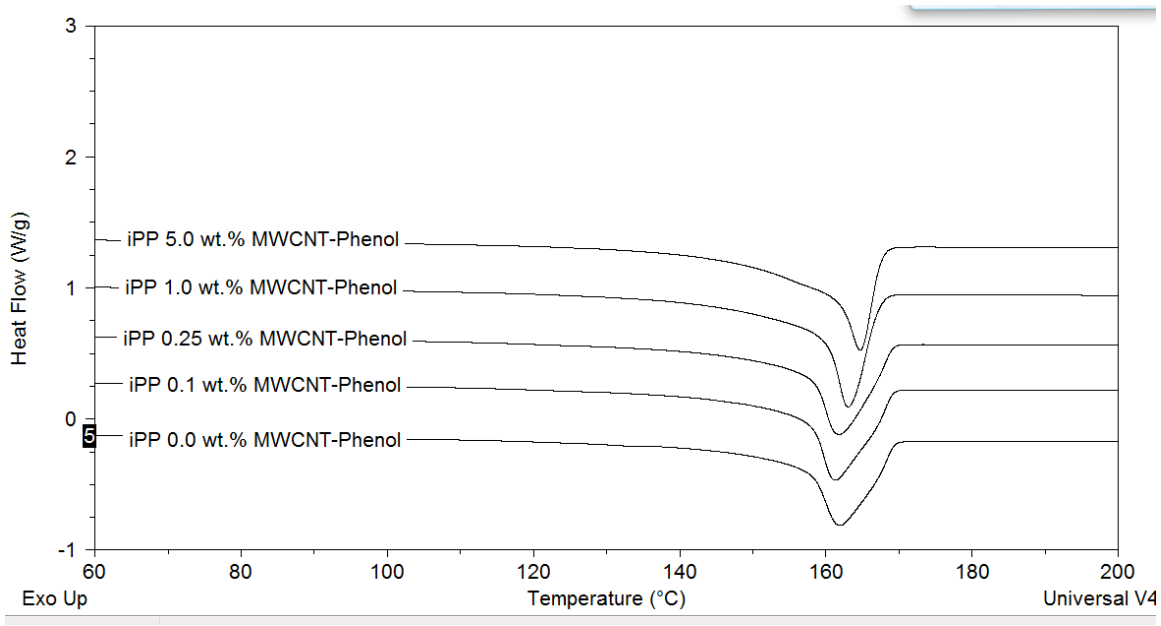

(f)

Figure 12: DSC thermograms of non-isothermal crystallization; (a) cooling peak of iPP/MWCNT-Phenol, (b) Melting peaks of iPP/MWCNT-Phenol

It is clear that, crystallization of neat iPP begins at a temperature much lower than the nanocomposites. Moreover, it can be seen from Fig. 10-12 that, the peak position of crystallization and melting curves reposition to a much more shorter region with incorporation of small amount of MWCNTs indicating enhanced overall crystallization and melting rate due to the nucleating effect of MWCNTs (Z. Wang 2008). Table 2 shows that the Pure iPP when cooled at 5°C min^{-1} crystallizes at 119.1 ◦C, while the crystallization in 0.25 wt.%, 1.0 wt.% and 5.0 wt.% Pure iPP/MWCNT

Table 3: Crystallization temperature (Tc), crystallization enthalpy ΔH (J/g), and the degree of crystallinity (Xc) of PP, PP/MWCNTs and PP/Phenol/MWCNTs nanocomposites.

Specimen	T_c (°C)	T_m (°C)	ΔH (J/g)	X_c (%)
iPP	119.1	161.1	97.0	44.8
0.1 wt.% iPP/MWCNT	122.1	161.9	96.3	46.1
0.25 wt.% iPP/MWCNT	125.9	164.4	96.5	46.3
1.0 wt.% iPP/MWCNT	129.4	165.3	102.0	49.3
5.0 wt.% iPP/MWCNT	132.1	165.9	98.8	49.8
0.1wt.% iPP/MWCNT-COOH	120.5	161.7	100.8	48.4
0.25wt.% iPP/MWCNT-COOH	121.0	162.0	103.7	49.4
1.0wt.% iPP/MWCNT-COOH	126.0	163.4	106.0	52.1
5.0wt.% iPP/MWCNT-COOH	130.7	164.8	108.9	54.8
0.1wt.% iPP/MWCNT-phenol	120.2	161.3	101.3	48.5
0.25wt.% iPP/MWCNT-phenol	120.2	161.8	103.6	49.7
1.0wt.% iPP/MWCNT-phenol	124.9	163.1	105.7	51.1
5.0wt. % iPP/MWCNT-phenol	128.4	164.7	103.5	52.1

nanocomposites are 125.9°C, 129.4°C and 132.1°C and the corresponding iPP/MWCNT-COOH and iPP/MWCNT-Phenol modified nanocomposites are 120.5°C, 121.0°C, 125.9°C, 130.7°C and 120.2°C, 124.9°C 128.4°C respectively.Moreover, the DSC measurement was used to determine the degree of crystallinity (X_c) of the composites (Table: 2). The X_c was evaluated from heat evolves during crystallization (ΔH_c) using the relationship:

$$X_c(\%) = \frac{\Delta H_c}{(1 - \text{wt.}\%)\Delta H_m} \times 100$$

Where ΔH_m is the heat of fusion for 100% crystalline isotropic iPP (ΔH_m = 209 J/g) and wt.% is the weight fraction of MWCNTs in the nanocomposites (Mark J. E. 1996). Earlier studies reported insignificant variation in the degree of crystallization (Funck and Kaminsky 2007) and (Zhang and Zang 2007) and a few reports suggest a decrease in crystallinity (Bao and Tjong 2008 and Jose et al 2007.).

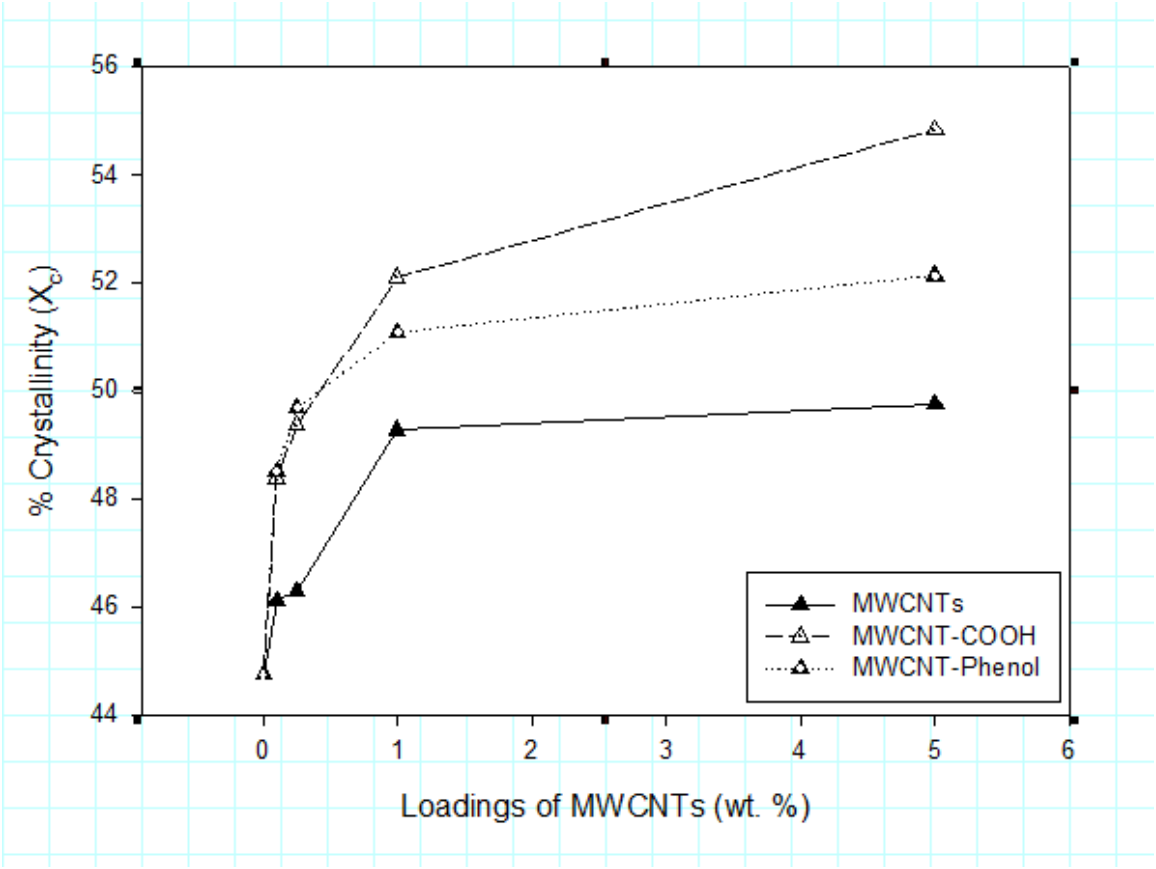

Figure 13: Percentage crystallinity of iPP/MWCNT, iPP/MWCNT-COOH and iPP/MWCNT-Phenol nanocomposites

Contrary to their observation, the present study (Fig 13) shows a distinct increase in the degree of crystallinity with addition of nanotubes into the iPP matrix which is in agreement with the results of (Tabuani et al. 2008; Li WH et al 2007)

4.2.2 Carbon Nanotubes Dispersion

In order to investigate the interaction and compatibility between MWCNTs with iPP chains and the morphology of the cross section and profile section of the composites, SEM was conducted on fractured surfaces of MWCNTs for 1.0 wt.% iPP/MWCNT, iPP/MWCNT-COOH and iPP/MWCNT-Phenol. The choice of 1.0 wt.% concentration of CNTs was stemmed from the highest mechanical properties was observed at 1.0 wt.% loading of CNTs in the polymer matrix coupled with considerable percentage elongation at brake. Fig. 14 shows the SEM images of MWCNT, MWCNT-COOH and MWCNT-Phenol as well images of their respective 1.0 wt.% CNT nanocomposites loadings.

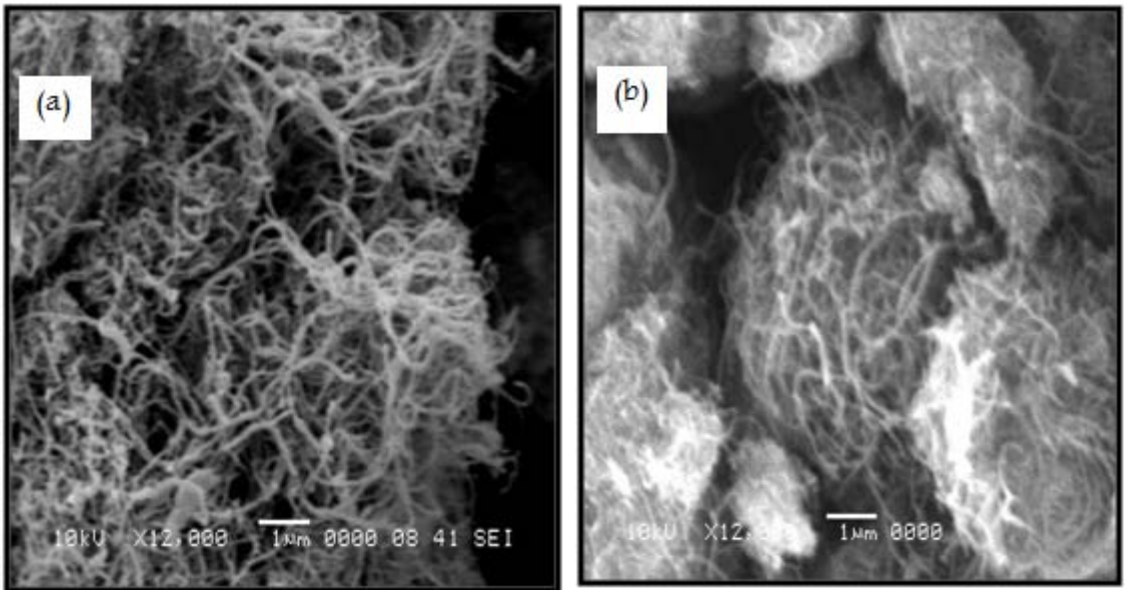

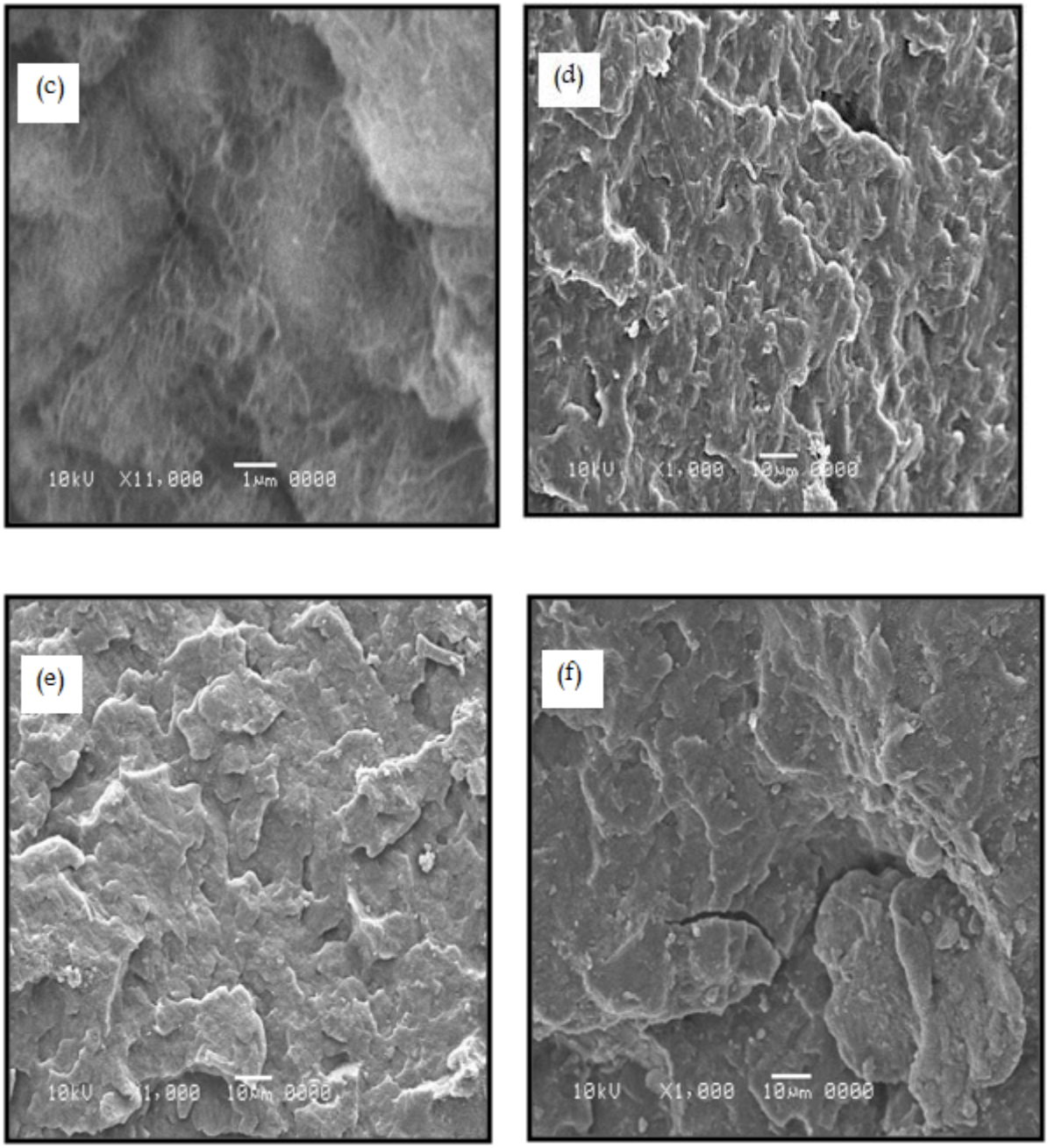

Figure 14: SEM picture of (a) MWCNT, (b) MWCNT-COOH, (c) MWCNT-Phenol and their corresponding iPP nanocomposites (d), (e) and (f) respectively

A uniform distribution of the nanotubes can be observed on different areas of the composite reinforced with MWCNT-Phenol than nanocomposites prepared with MWCNT or MWCNT-COOH. Moreover less agglomeration is observed on different location of composite prepared with MWCNT-COOH than those of pure MWCNTs. These can be attributed to the good dispersion tendency of modified nanotubes over the non-modified counterpart.

4.2.2 Mechanical Characterization

The mechanical properties of iPP in comparison to iPP/MWCNT, iPP/MWCNT-COOH and iPP/MWCNT-Phenol are reported in the Table 3. It can be seen from these results that MWCNT-Phenol has remarkable reinforcing effect on the mechanical properties of iPP compared to Pure MWCNT and functionalized MWCNT-COOH. It is obvious that the Young's Modulus and the maximum stress of these materials were highly enhanced with the modified CNTs compared to the unmodified CNTs. The Young's Modulus and Tensile Stress increases with increase in CNTs proportion in the composite for either type of nanotubes as represented in Fig. 15. The percentage increase in modulus of iPP/MWCNT-Phenol rises from 60.85% at 0.25 wt.% MWCNT-Phenol loading to as higher as 107.40% at 1.0 wt.% MWCNT-Phenol whereas for iPP/MWCNT and iPP/MWCNT-COOH it increases respectively from 51.45% to 77.96% and 26.15% to 30.95% for the same nanotubes loading.

Table 4: Summary of mechanical properties of neat iPP and PP/MWCNTs composites sample as a function of Nanotubes loading.

Sample	Modulus (MPa)	Maximum Stress (MPa)	% Elongation at Break	% increase in Modulus
iPP	713.1	35.97	26.12	-------
0.1 wt.% iPP/MWCNT	810.0	35.90	18.66	13.59
0.25 wt.% iPP/MWCNT	899.6	37.27	16.36	26.15
1.0 wt.% iPP/MWCNT	933.8	38.76	10.07	30.95
5.0 wt.% iPP/MWCNT	986.3	43.11	8.07	38.31
0.1wt.% iPP/MWCNT-COOH	852.2	37.08	20.48	19.51
0.25wt.% iPP/MWCNT-COOH	1080.0	38.08	19.64	51.45
1.0wt.% iPP/MWCNT-COOH	1269.0	38.27	8.55	77.96
5.0wt.% iPP/MWCNT-COOH	1277.0	41.43	6.08	79.07
0.1wt.% iPP/MWCNT-phenol	909.5	39.52	19.99	27.54
0.25wt.% iPP/MWCNT-phenol	1147.0	40.28	16.09	60.85
1.0wt.% iPP/MWCNT-phenol	1479.0	43.76	13.21	107.40
5.0wt. % iPP/MWCNT-phenol	1395.0	45.04	6.51	95.62

However, it is interesting to note that the modulus of Phenol Modified MWCNTs/PP decrease from 1479MPa at 1.0 wt.% MWCNTs loading to 1395MPa at 5.0 wt.% loading of nanotubes. These however is due to agglomeration of CNTs at higher loadings (5.0 wt.%). Similar phenomena was reported in (Valentini et al. 2003 and Goh et al. 2008) for as low as 1.0 wt.% iPP/SWCNTs and iPP/grafted MWCNTs composites respectively. In the case of iPP/MWCNTs and iPP/MWCNT-COOH composite, a relative increase in the tensile properties was observed for the different concentration of nanotubes.

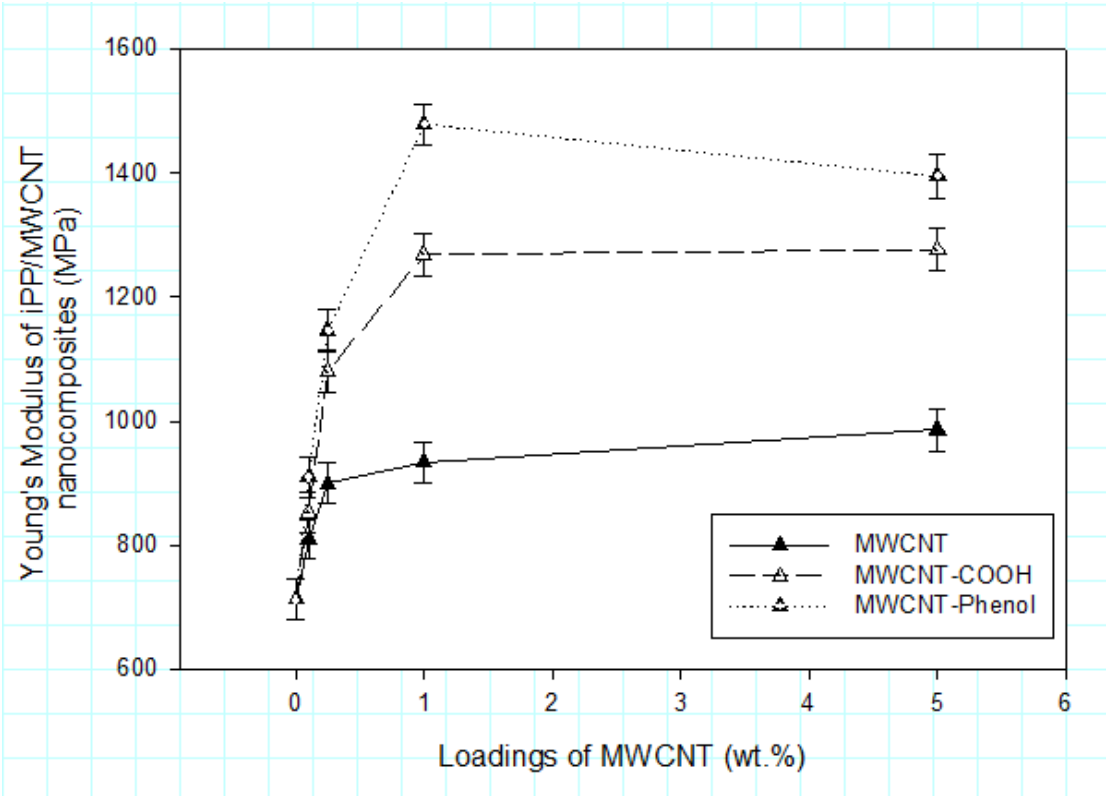

Figure 15: Young's Modulus of iPP/MWCNT, MWCNT-COOH and MWCNT-phenol modified composites

The tensile properties are more enhance with addition of MWCNT-Phenol at all nanotubes loadings followed by MWCNT-COOH and MWCNTs. In addition, 1.0 wt.% loading of MWCNT-Phenol which correspond to the highest Young's Modulus gives minimum reduction in percentage elongation at brake compared to the same loadings for MWCNT-COOH and MWCNT. These improvements arises from the fact that both MWCNT-Phenol and MWCNT-COOH promotes uniform distribution and dispersion of MWCNTs into the iPP matrix and prevent agglomeration of the filler particles that tend to form clusters due to van der Waals attraction forces as seen from the SEM images in

Fig. 14. Moreover, it is widely agreed that good dispersion of MWCNTs enable more efficient load transfer from the polymer matrix to the nanofillers (Blake et al. 2006 and Yang et al. 2007) thus higher improved mechanical properties are obtained from the functionalized CNTs.

4.2.3 Effect of MWCNT-Phenol Conclusion

The effects of surface modifications of MWCNTs on the mechanical and thermal properties iPP matrix were investigated for -COOH and -phenolic functional groups. The study shows greater dispersion and lesser aggregates of MWCNT-phenol followed by MWCNT-COOH and pure MWCNTs. A significant improvement of tensile stress, Young's Modulus of iPP reinforced with modified MWCNTs over the non-modified MWCNTs was achieved. The highest percentage increase in Young's modulus was recorded at 1.0 wt.% loading of MWCNT-phenol followed by MWCNT-COOH and unmodified MWCNTs. Both the tensile properties and percentage crystallization found to increase with increasing concentration of MWCNTs. However, it is interesting to note that the % crystallinity was higher in the case of iPP/MWCNT-COOH followed by iPP/MWCNT-phenol and iPP/MWCNT.

4.3 EFFECT OF 1-OCTADECANOL MODIFICATION ON THERMAL AND MECHANICAL PROPERTIES OF POLYPROPYLENE/CNT NANOCOMPOSITES

4.3.1 Nucleation Behavior and Thermal Analysis of iPP/MWCNT-C_{18} nanocomposites

Non isothermal DSC was used to investigate the effect of crystallization of iPP matrix filled with MWCNT-C_{18} at a cooling rate of 5 °C min^{-1}. Fig 16 shows the DSC thermograms obtained for iPP/MWCNT-C_{18} and compared to thermograms of iPP/MWCNT and iPP/MWCNT-COOH in Figure 10 and 11 above. It is obvious that crystallization of iPP begins at a temperature much lower than iPP/MWCNT composites as well as the modified iPP/MWCNT-COOH and iPP/MWCNT- C_{18} nanocomposites.

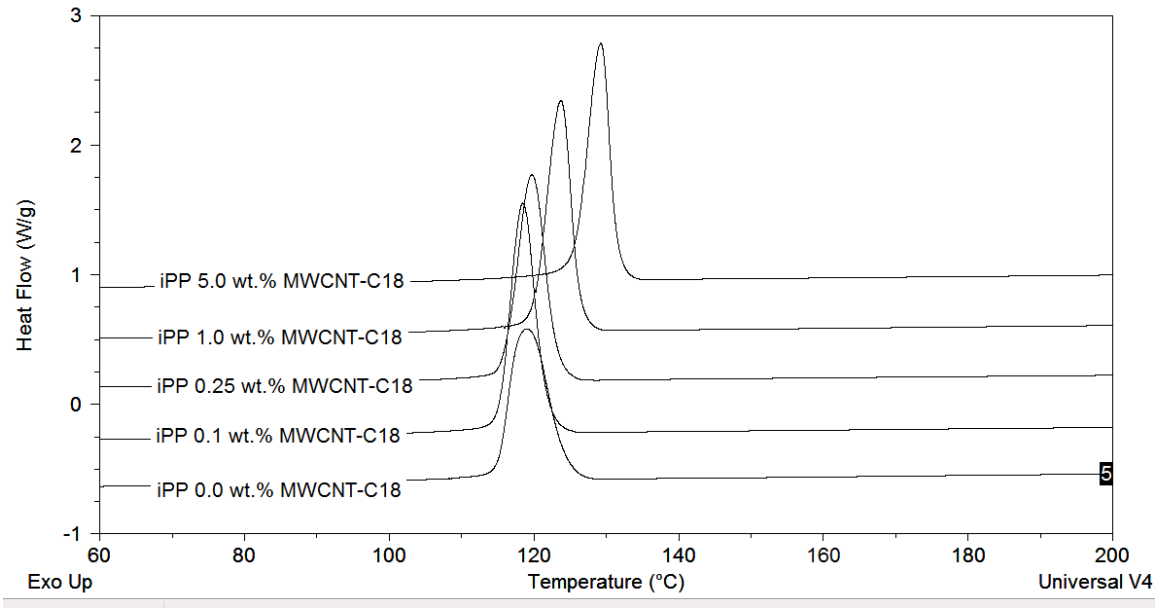

(a)

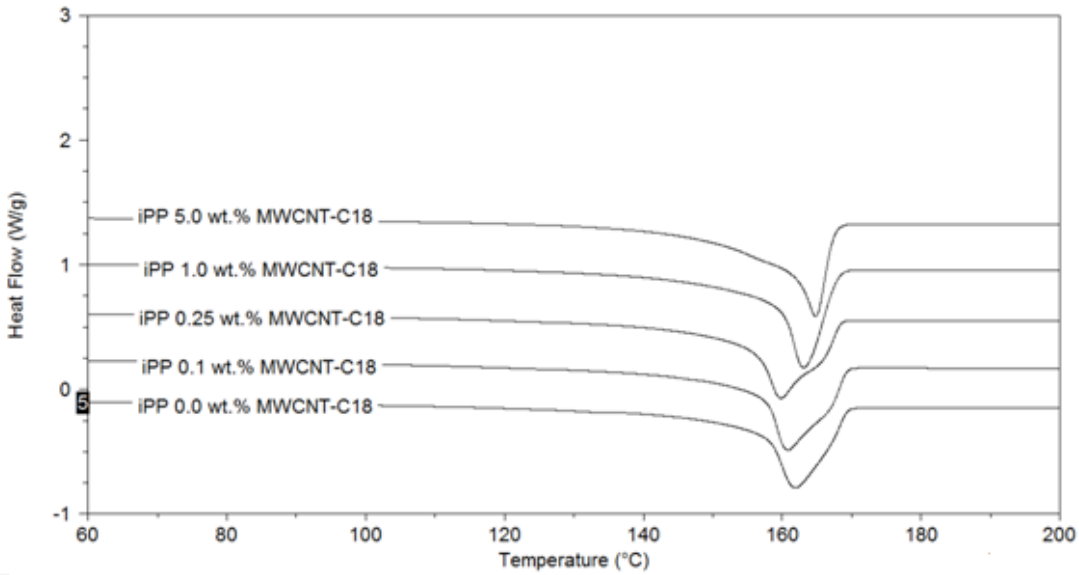

Figure 16: DSC thermograms of non-isothermal crystallization; (a) cooling (b) melting peaks of iPP/MWCNTC-18 nanocomposites.

(b)

Moreover it can seen from Fig 16 that the peak position of crystallization and melting curves reposition to a much more shorter region with incorporation of small amount of CNTs indicating enhanced overall crystallization and melting rate due to nucleating effect of CNTs. (Z. Wang 2008). Table 4 shows that the iPPMWCNT-C18 nanocomposites when cooled at 5C min^{-1} crystallizes at 119.0 ºC for 0.1 wt.% loading and 120.0 ºC for 0.25 wt.% loading of MWCNT-C18. These increment is however insignificant compares to iPP matrix, iPP/MWCNT-COOH and iPP/MWCNT-phenol (Table 3). However, at 1.0 and 5.0 wt.% loading of MWCNT-C18, the percentage of crystallinity increases insignificantly above it value at 0.1 loading. This phenomenon of increase, decrease then increase was reported in Boa and Tjong et al 2008.

Table 5: Crystallization temperature (Tc), crystallization enthalpy ΔH (J/g), and the degree of crystallinity (Xc) of iPP/MWCNT-C18 nanocomposites.

Specimen	Tc (°C)	Tm (°C)	ΔH (J/g)	Xc (%)
0.1wt.% iPP/MWCNT-C_{18}	118.5	160.9	102.2	49.0
0.25 wt.% MWCNT-C_{18}	119.7	159.9	99.8	47.9
1.0wt.% iPP/MWCNT-C_{18}	123.7	163.1	98.8	47.8
5.0wt.% iPP/MWCNT-C_{18}	129.2	164.9	97.4	49.0

In addition, the degree of crystallinity of iPP/MWCNT-C18 nanocomposites was determined from the DSC measurement using equation 1. The X_c as evaluated from heat evolves during crystallization (ΔH_c) was shown in Table 3

Figure 17 shows the percentage crystallinity as a function of nanotube loadings. It can be seen that there is a sharp increase in Xc at 1.0 wt.% MWCNT-C18 loading, however, with subsequent loadings of 0.25 and 1.0 wt.% the percentage crystallinity drastically reduced to 48.7 and 48.9 respectively before it again raises up to 49.0 at 5.0 wt.% loadings. This trend was however not observed in iPP/MWCNT and iPP/MWCNT-COOH in Figure 13.

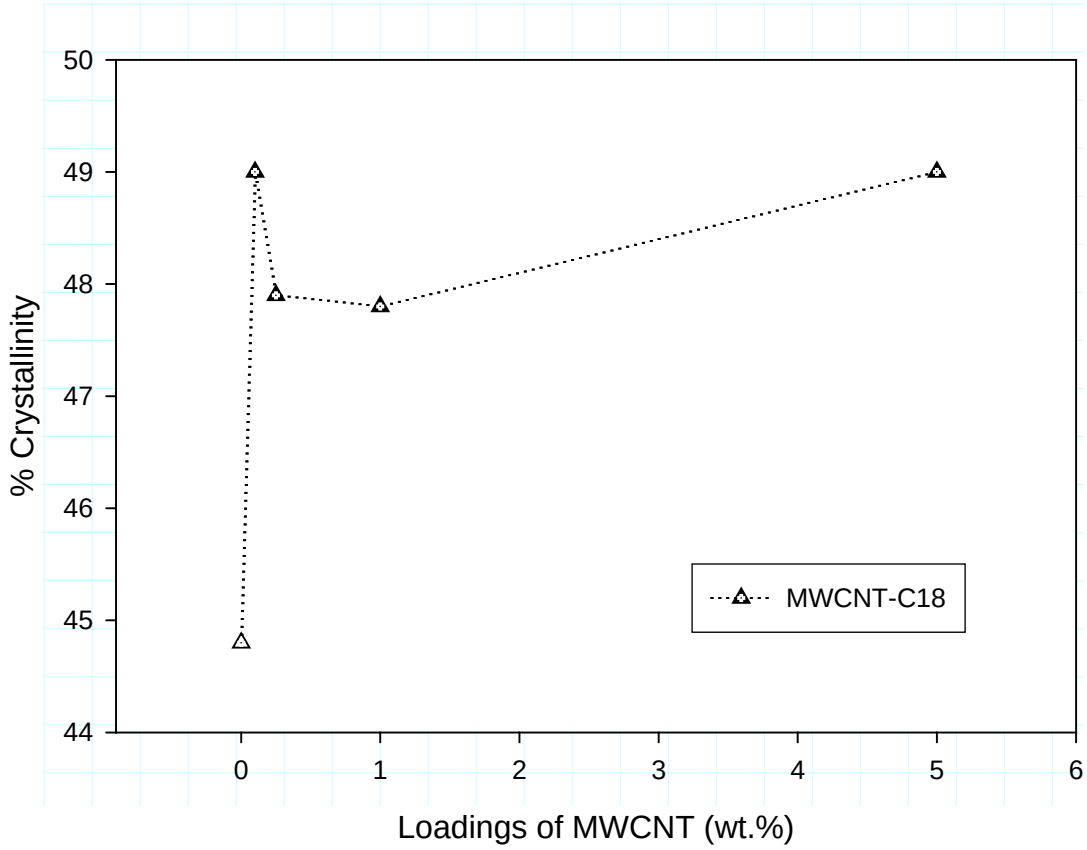

Figure 17: Percentage crystallinity of iPP/MWCNT-C18 nanocomposites

For example, between 1.0 wt.% and 5.0 wt.%, the percentage crystallization of iPP/MWCNT and iPP/MWCNT-COOH increases from 49.28 to 49.75 and 52.10 to 54.84 respectively. An overall increase in degree of crystallinity was observed as reported in (Tabuani et al. 2008; Li WH et al 2007). Interestingly, however, crystallization of iPP/MWCNT- C_{18} nanocomposites and recorded an insignificant variation in overall degree of crystallization (Funck and Kaminsky 2007). Although the enhancement effect of the CNTs on the nucleation rate iPP was observed from the CNTs of either type by the

repositioning of their DSC thermograms, a slight decrease in percentage crystallinity was noticed in the case of iPP/MWCNT- C_{18}. The percentage crystallinity increases with addition 0.1 wt.% MWCNT- C_{18}, it however decreases at 0.25 wt.% and 1.0 wt.% MWCNT- C_{18}. These were report of (Bao and Tjong 2008; Jose et al 2007).

4.3.2 Dispersion of CNTs

The interaction and compatibility of the CNTs in iPP matrices and the morphology of the cross section and profile section of the nanocomposites was investigated. For this purpose, SEM was conducted on fractured surfaces of the nanocomposites for 1.0 wt. % iPP/MWCNT- C_{18} (Figure 18) and compared to images of figure 1X and 1B of iPP/MWCNT and iPP/MWCNT-COOH respectively. Moreover, as stated earlier, the choice of 1.0 wt.% loading of CNTs was stemmed from the facts that nanotubes at 1.0 wt.% gives the highest mechanical properties in all the nanocomposites. Fig 18 shows the SEM image of iPP/MWCNT-C_{18} nancomposite. Although, different fractured surface of the composites were scanned for SEM, there was however no clear disparity between the image of iPP/MWCNT-C_{18} and images obtained for iPP/MWCNT and iPP/MWCNT-COOH in Figure 14 (d) and 14 (e) above. Carbon nanotubes were not observed from these images. It can be assumed that the MWCNT involved were of poor quality, hence the assumption that all the CNTs imbedded in the matrix were fractured during SEM sample preparation. However, there is a clear difference between the fractured surface of iPP/MWCNT-C18 nanocomposites (Figure 18) and the nanocomposites of iPP/MWCNT, iPP/MWCNT-COOH and iPP/MWCNT-phenol. (Figure 14). In these case, iPP/MWCNT-C18 forms chunks and clusters might be the reason for non-enhancement

in mechanical properties of the iPP/MWCNT- C_{18} as compared to the preceding nanocomposites.

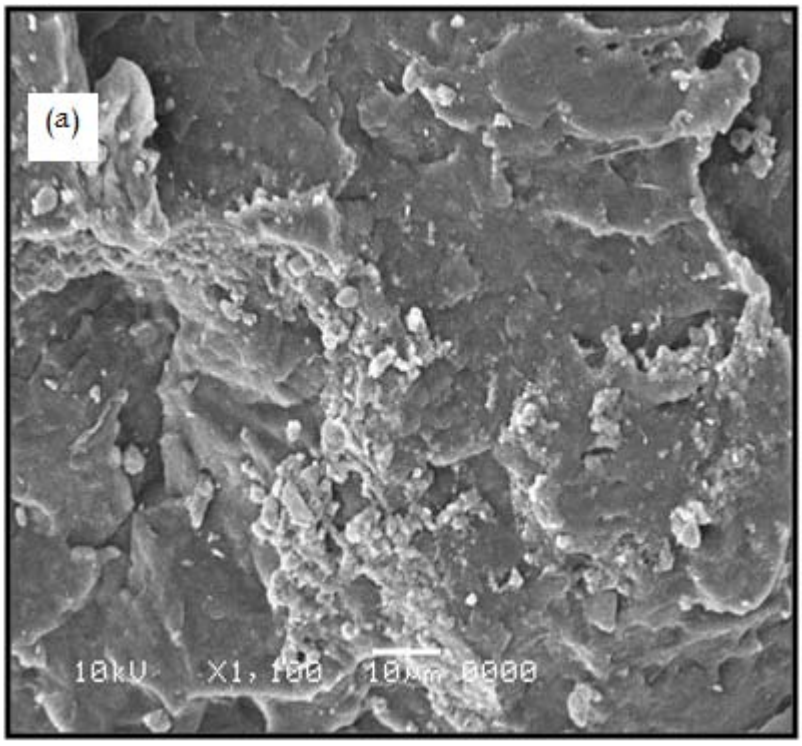

Figure 18: SEM image of 1.0 wt.% iPP/MWCNT-C18 nanocomposites

4.3.3 Mechanical Characterization

The mechanical properties of iPP/MWCNT- C_{18} were reported in Table 6 and compared with properties of iPP/MWCNT and iPP/MWCNT-COOH in Table 4. It can be seen from these results that above 0.1 wt.% loadings, the nanotubes modified by octadecanol (C_{18}) has no remarkable effect on the mechanical properties of iPP compared to pure iPP/MWCNT and iPP/MWCNT-COOH. The modulus of iPP/MWCNT-C C_{18} was

increased by 15.50 % at 0.1 wt.% loading of MWCNTs. It however decreases at subsequent loadings, i.e. 0.25, 1.0 and 5.0 wt.% loadings of MWCNT- C_{18}. Fig 19 represents the Young's modulus as a function of nanotubes loadings.

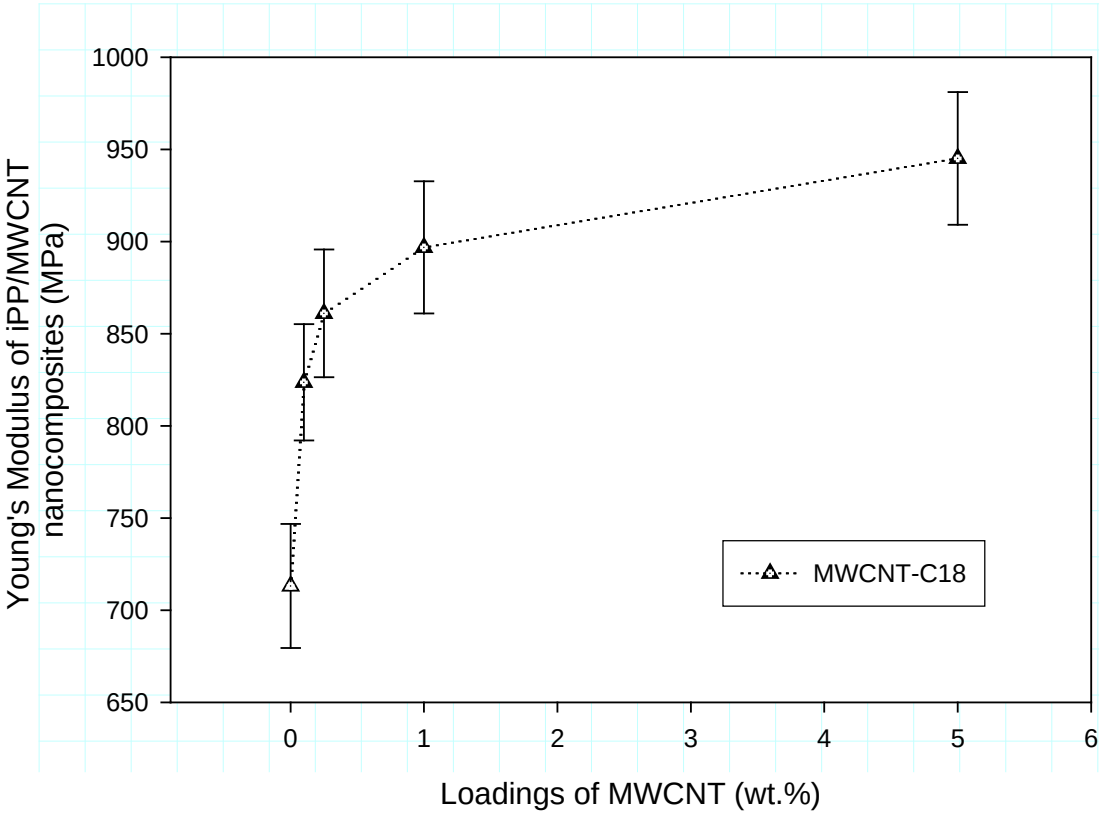

Figure 19: Young's modulus of iPP/MWCNT-C18 nanocomposites

It is obvious from Fig 19 that the Young's modulus of iPP/MWCNT- C_{18} was enhanced above the unmodified CNTs only at 0.1 wt.% nanotubes loading compared to unmodified iPP/MWCNT nanocomposites in Figure 15. Increased in the MWCNT- C_{18} content into the iPP matrix increases the Modulus of iPP/MWCNT- C_{18} composites but this increase

is however below the reinforcing effect the unmodified iPP/MWCNT composites. Though, the overall trend shows that the Young's modulus increases with increase in nanotubes loading, it is however very clear that MWCNT- C_{18} overall enhancement was below that of unmodified iPP/MWCNTs. This unexpected phenomenon can be explain from the fact that MWCNT- C_{18} forms larger chunks which results into clusters on the fractured surface and hence give rise to potentials of formation of aggregates as shown in the SEM image of Figure 18. The MWCNT- C_{18} might instead be dispersed in bundles, thus resulting into formation large agglomerates subsequently, decline of enhancing ability of MWCNT- C_{18} even below the MWCNT.

Table 6: Summary of mechanical properties of iPP/MWCNT-C18 nanocomposites as a function of Nanotubes loading

Sample	Modulus (MPa)	Maximum Strength (MPa)	Elongation at Break (%)	Increase in Modulus (%)
0.1wt.% iPP/MWCNT-C_{18}	823.6	37.3	23.0	15.5
0.25 wt.% MWCNT-C_{18}	861.0	37.7	20.1	20.7
1.0wt.% iPP/MWCNT-C_{18}	896.8	38.4	10.9	25.8
5.0wt.% iPP/MWCNT-C_{18}	945.1	39.2	7.02	32.5

4.3.4 Effect of MWCNT-C18 Conclusion

The effects of surface modifications of MWCNT on the mechanical and thermal properties iPP matrix were investigated for iPP/MWCNT–C_{18} nanocomposites. The SEM

image clusters and chunks on the fractured surface, thence potential for aggregate and lesser dispersion in iPP/MWCNT-C_{18} matrix compared both iPP/MWCNT and iPP/MWCNT-COOH. Though a significant improvement in tensile stress, Young's modulus of iPP reinforced with modified MWCNT- C_{18} was observed at 0.1 wt.% loading of the modified CNT, it however falls below the reinforcing ability of the unmodified nanotubes. Both the tensile properties and percentage crystallization were found to increase with increasing concentration of MWCNT. It is interesting to note that the % crystallinity was higher in the case of iPP/MWCNT-COOH followed, there was however no different between the % crystallinity of iPP/MWCNT and iPP/MWCNT- C_{18}.

4.4 EFFECT OF DODECYLAMINE MODIFICATION ON THERMAL AND MECHANICAL PROPERTIES OF POLYPROPYLENE/CNT NANOCOMPOSITES

4.4.1 Nucleation behavior and thermal analysis of iPP/MWCNT-amine nanocomposites

Non isothermal DSC was used to investigate the effect of crystallization of PP matrix filled with MWCNT-Amine at a cooling rate of. Figure 20 shows the dynamic thermograms obtained for iPP/MWCNT-amine at a cooling rate of 5 °C min^{-1} and compared with the thermograms of iPP/MWCNT and iPP/MWCNT-COOH from Figure 10 and 11. It is obvious that unlike MWCNT and MWCNT-COOH, there is no remarkable influence of MWCNT-amine on the crystallization temperature of iPP matrix.

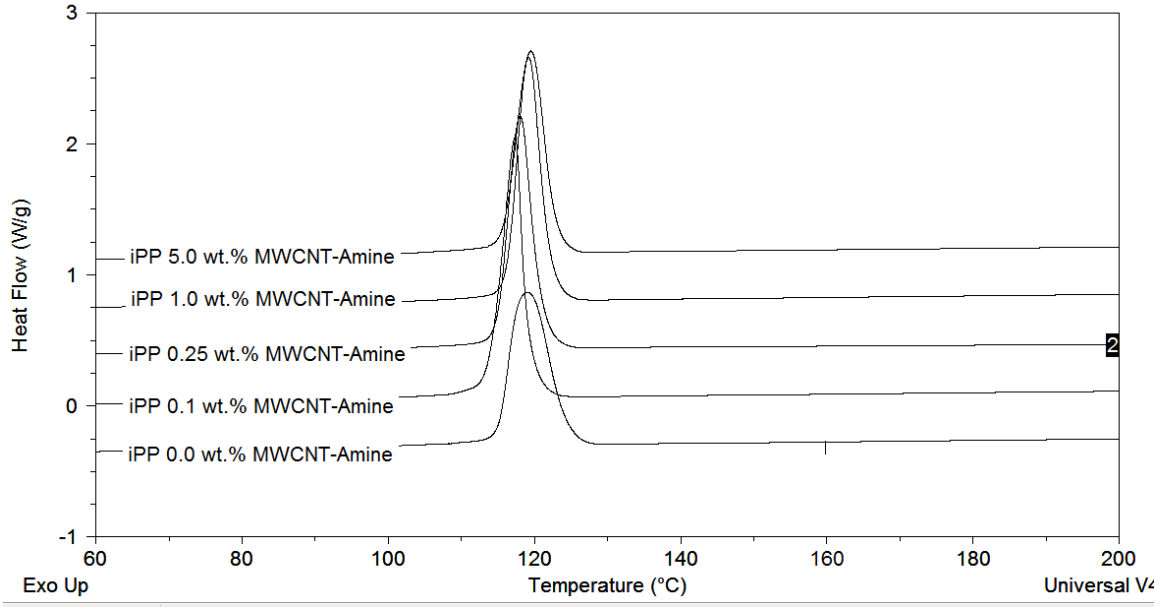

(a)

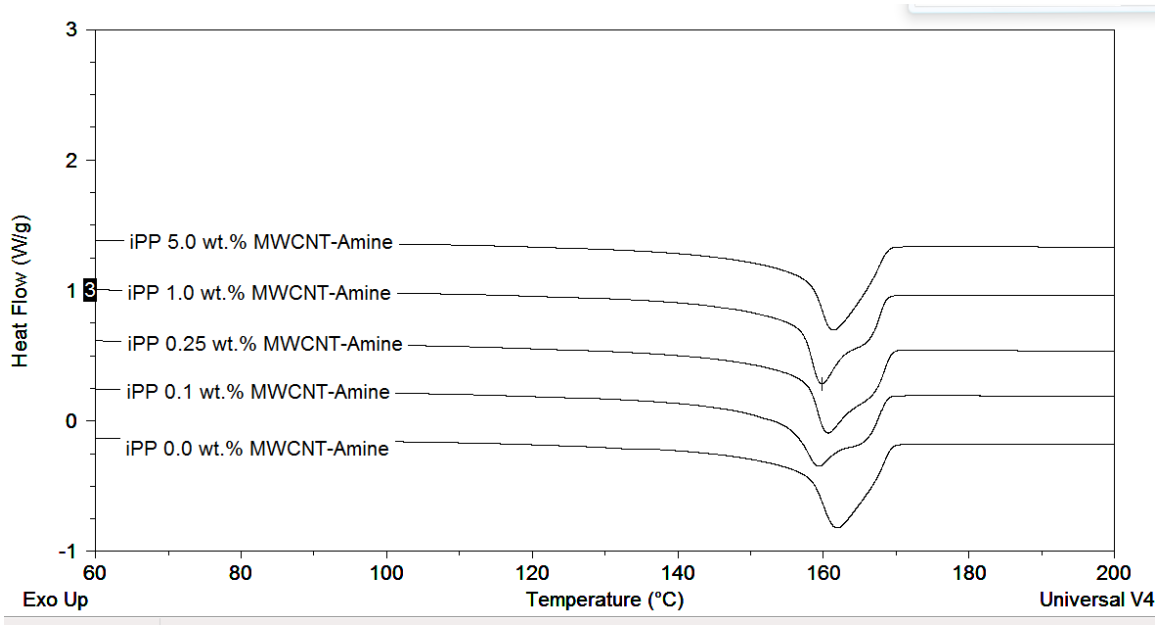

(b)

Figure 20: DSC thermograms of non-isothermal crystallization; (a) cooling and (b) Melting peaks of iPP/MWCNT-amine

Moreover it can seen from Fig 20 that there is no much shifting in peak position of crystallization and melting curves of iPP/MWCNT-amine nanocomposites as compared to MWCNT and MWCNT-COOH which in each case reposition to a much more shorter region with incorporation of small amount of CNTs indicating enhanced overall crystallization and melting rate due to nucleating effect of CNTs. (Z. Wang 2008).

From Table 3 it was seen that iPP when cooled at 5 °Cmin-1 crystallizes at 119.1 ºC while the crystallization of 0.25 wt.%, 1.0 wt. % and 5.0 wt.% iPP/MWCNT composites are 125.8 ºC, 129.4 ºC, 132.1 ºC and their corresponding modified iPP/MWCNT-COOH

120.5 ºC, 125.9 ºC, 130.7 ºC C. however, Table 7 shows lower crystallization temperature of iPP/MWCNT-amine at all loadings compared to iPP/MWCNT and iPP/MWCNT-COOH.

Table 7: Crystallization temperature (Tc), crystallization enthalpy ΔH (J/g), and the degree of crystallinity (Xc) of iPP/MWCNT-amine nanocomposites.

Specimen	T_c (°C)	T_m (°C)	ΔH (J/g)	X_c (%)
0.1 wt.% iPP/MWCNT-amine	117.2	154.4	106.4	51.0
0.25 wt.% iPP/MWCNT-amine	118.0	160.7	99.5	47.7
1.0 wt.% iPP/MWCNT-amine	119.2	159.9	100.3	48.5
5.0 wt. % iPP/MWCNT-amine	119.5	161.3	96.3	48.5

In Figure 13, the iPP/MWCNT and iPP/MWCNT-COOH shows significant increase in percentage crystallinity. In both cases, the crystallization increases with addition of CNTs. For example, between 1.0 wt.% and 5.0 wt.%, the percentage crystallization of iPP/MWCNT and iPP/MWCNT-COOH increases from 49.3 to 49.8 and 52.1 to 54.8% respectively. However, Figure 21 MWCNT-amine depicts no increase within the same range. An overall increase in degree of crystallinity was observed in iPP/MWCNT and iPP/MWCNT-COOH as reported in (Tabuani et al. 2008; Li WH et al 2007).

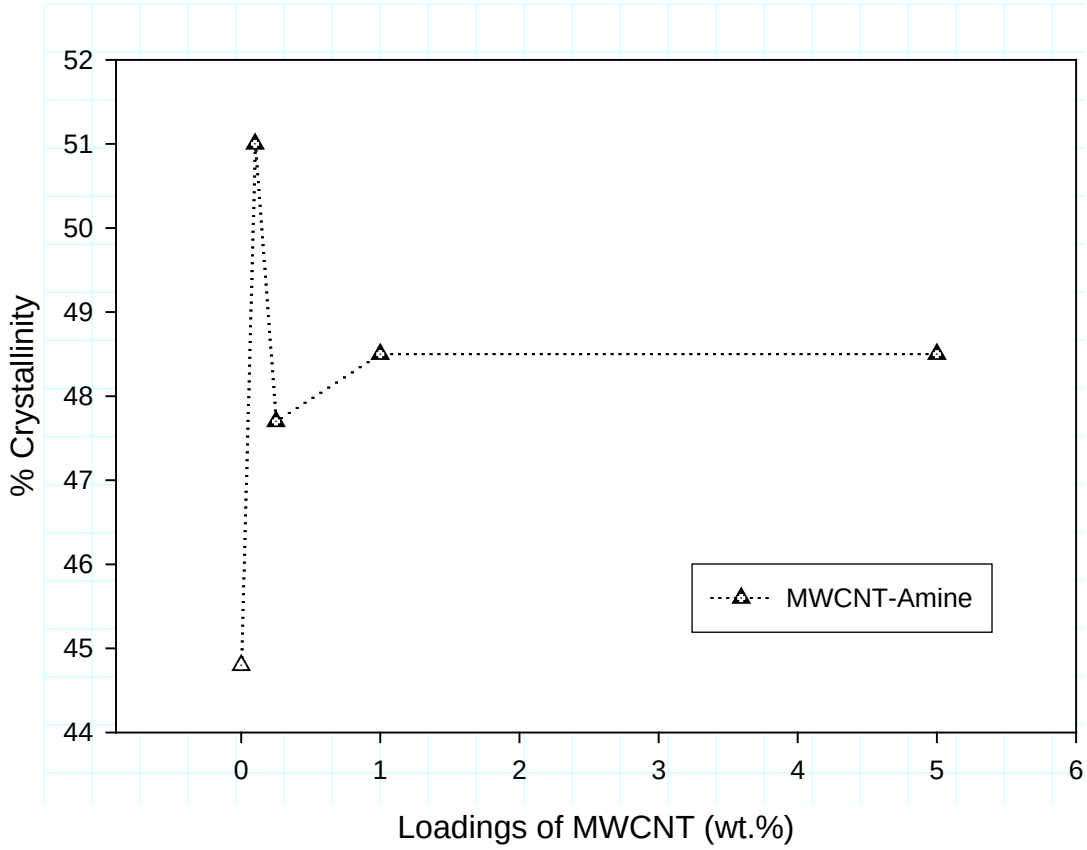

Figure 21: Percentage crystallinity of iPP/MWCNT-amine nanocomposites

Interestingly, however, crystallization of iPP/MWCNT-amine nanocomposites recorded insignificant variation in overall degree of crystallization as reported in Funck and Kaminsky 2007. Moreover MWCNT-amine gave no enhancement effects on the nucleation rate of iPP matrix. Aside the slightest increase in percentage crystallinity at 0.1 wt.% MWCNT-amine, the overall percentage crystallinity decrease with addition of MWCNT-amine as reported in Bao and Tjong 2008 as well as Jose et al 2007.

4.4.2 Dispersion of CNTs

Fig 22 shows the SEM image of iPP/MWCNT-amine. This moreover when compared to the images of figure 14(d) and 14(e) of iPP/MWCNT and iPP/MWCNT-COOH shows clear difference of the influence different surfactants on the morphology of the fractured surface of iPP matrix. Moreover, as stated earlier, the choice of 1.0 wt.% loading of CNTs was stemmed from the facts that nanotubes at 1.0 wt.% gives the highest mechanical properties in all the nanocomposites. Although, different fractured surface of the composites were scanned for SEM, there was however no clear disparity between the image of iPP/MWCNT-amine and images obtained for iPP/MWCNT and iPP/MWCNT-COOH in Figure 14 above. Carbon nanotubes were not observed from these images. It can be assumed that the MWCNT involved were of poor quality, hence the assumption that all the CNTs imbedded in the matrix were fractured during SEM sample preparation. However, there is a clear difference between the fractured surface of iPP/MWCNT-amine nanocomposites (Figure 22) and the nanocomposites of iPP/MWCNT, iPP/MWCNT-COOH and iPP/MWCNT-phenol. (figure 14). In this case, iPP/MWCNT-amine forms fiber-like matrix with chunks and clusters which might be the rationale for non-enhancement in mechanical properties of the iPP/MWCNT-amine as compared to the preceding nanocomposites.

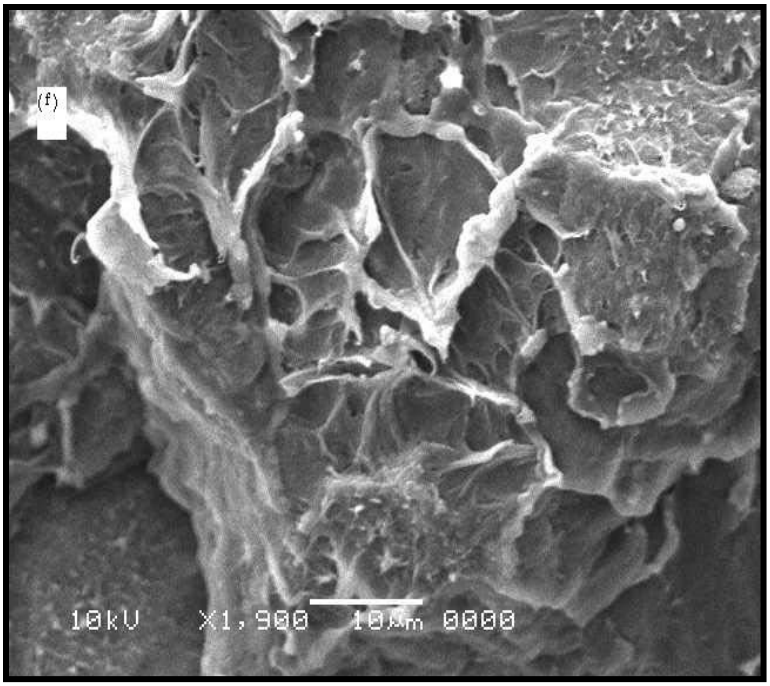

Figure 22: SEM image iPP/MWCNT-amine nanocomposites

4.4.3 Mechanical Characterization

The mechanical properties of iPP/MWCNT-amine were reported in Table 8 and compared to iPP/MWCNT and iPP/MWCNT-amine. It can be seen from these results that above 1.0 wt.% loadings, the nanotubes modified by dodecylamine (-amine) has no remarkable effect on the mechanical properties of iPP compared to pure iPP/MWCNT and iPP/MWCNT-COOH. The Young's modulus of iPP/MWCNT-amine increased by 14.7 % at 0.1 wt.% loading of MWCNTs. It however increases little below the unmodified iPP/MWCNT nanocomposite with subsequent loadings, i.e. 0.25, 1.0 and 5.0 wt.% loadings of MWCNT-amine. Fig 23 represents the Young's Modulus as a function of nanotubes loadings.

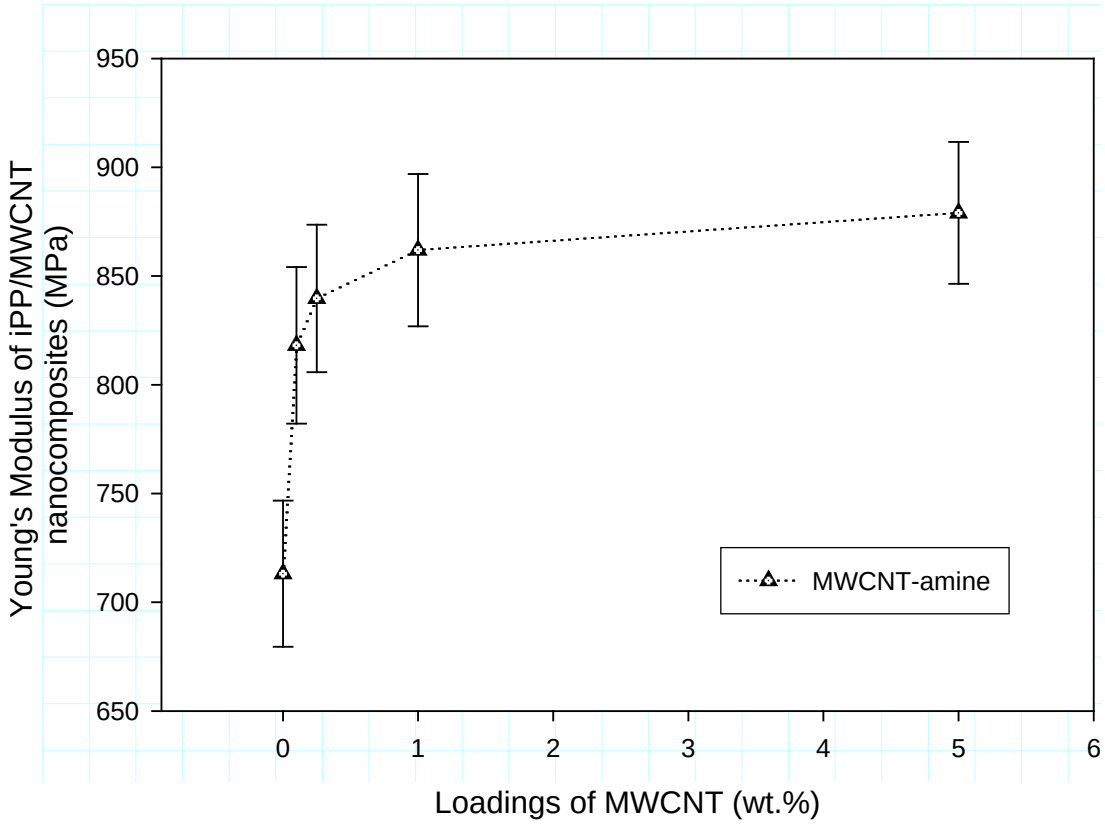

Figure 23: Young's Modulus of iPP/MWCNT-amine nanocomposites

From Fig 23 above, it is obvious that the extent of enhancement of the Young's modulus of iPP/MWCNT-amine is only 1.1% above the unmodified iPP/MWCNT nanocomposites at 0.1 wt. % loadings of the CNTs into iPP matrix. Although increased in the MWCNT-amine content into the iPP matrix increases the Modulus of iPP/MWCNT-amine nanocomposites, this increased is however below the reinforcing effect the unmodified iPP/MWCNT composites. Though, the overall trend shows that the Young's

modulus increases with increase in nanotubes loading, it is however very clear that MWCNT-amine overall enhancement was below that of unmodified iPP/MWCNT.

Table 8: Summary of mechanical properties of neat iPP and iPP/MWCNT nanocomposites as a function of Nanotubes loading

Samples	Modulus (MPa)	Maximum Strength (MPa)	Elongation at Break (%)	Increase in Modulus (%)
0.1 wt.% iPP/MWCNT-amine	818.1	37.1	9.1	14.7
0.25 wt.% iPP/MWCNT-amine	839.7	32.3	8.0	17.8
1.0 wt.% iPP/MWCNT-amine	861.9	36.6	7.6	20.9
5.0 wt. % iPP/MWCNT-amine	879.0	37.8	6.3	23.3

This phenomenon can be explain from the fact that MWCNT-amine forms chunks which results into cluster of aggregates as shown in the SEM image of Fig 22. The MWCNT-amine was instead dispersed in bundles and forms large agglomerates that results in the decline of enhancing ability of MWCNT-amine even below the pure MWCNT.

4.4.5 Effects of MWCNT-amine Conclusion

The effects of surface modifications of MWCNTs on the mechanical and thermal properties iPP matrix were investigated for iPP/MWCNT–amine nanocomposites. The SEM image of iPP/MWCNT-amine shows fiber-like-chunked fractured surface hence a potential for aggregate and lesser dispersion in MWCNT-amine matrix compared both

MWCNT and MWCNT-COOH. Though a significant improvement in tensile strength Young's Modulus of iPP reinforced with modified MWCNT-amine was observed at 0.1 wt.% loading of the modified CNT, it however falls below the reinforcing ability of the unmodified nanotubes. Both the tensile properties and percentage crystallization were found to increase with increasing concentration of MWCNT. It is interesting to note that the percentage crystallinity was higher in the case of iPP/MWCNT-COOH followed, there is however not much different between the % crystallinity of iPP/MWCNT and iPP/MWCNT-amine.

CHAPTER 5

5 CONCLUSIONS AND RECOMMENDATIONS

5.1 CONCLUSIONS

The effects of different surfactant on the surface modification of CNTs and on the thermal and mechanical properties of iPP nanocomposites have been investigated. The study shows Phenol and carboxylic acid modification gave significant improvement of both mechanical and thermal properties of iPP matrix. Modification by dodecylamine and octadecanol gave enhanced mechanical properties at 0.1 wt.% loading of CNT beyond which the mechanical properties decreases. On the other hand, modification by phenol and COOH gave highest tensile strength, the Young's modulus and reasonable percentage elongation at brake at 1.0 wt.% loading of CNTs. This value is however higher than the 0.75 wt.% threshold value reported in the existing literatures. Moreover, the SEM images better fractured morphology in order of -phenol, -COOH, -C18 and –amine which correspond to the order of superiority in mechanical properties. However, in all cases, a conclusive remarks cannot be drawn due to inability of the images to pictured the carbon nanotubes from the matrix.

On the other hand, the degree of crystallinity increases with increasing CNTs loading into the matrix except for amine which shows relatively no changes in degree of crystallinity with little or no nucleating effect with increase in CNT loadings. The group –COOH gave the highest percentage crystallinity followed by –Phenol, -C18 and amine group.

5.2 RECOMMENDATIONS

The effects of nanotubes modification using carboxylic, phenolic, amine and octadecanol on the properties of iPP/CNT nanocomposites have been developed. Despite enhanced improvement of dispersion, mechanical and thermal properties of the iPP matrices, there is still more rooms for understanding of the effect of these surfactants on other properties the polymer nanocomposites. Moreover, even though there is enhancement in dispersion and mechanical properties of iPP through nanotubes functionalization, there are still challenges and opportunities required to overcome in order to translate fully the unique properties of CNTs into the polymer matrices. Some of these opportunities and challenges are recommended as follows:

1. There is need for a method of attaining a specific and controlled functionalization as well as optimal functionalization of the CNTs for strong interfacial adhesion between CNTs and a given iPP matrix, which may also simultaneously improve the dispersion of CNTs in the iPP matrix.
2. There is also a need for TGA study in other to ascertain quantitatively the extent to which the surfactants are grafted on the CNTs.
3. Rheological studies to determine the effects of these surfactants on the iPP composite flow properties, including properties changes with temperature and deformation rates.

4. The use of compatibilizer such as PP-grafted mealic anhydrides to reduce interfacial energy between the composite materials in order to increase adhesion, finer dispersion, as well as to obtain more regular and stable composite morphology.
5. Future studies should also include the use of DMA to determine how these surfactants influence the viscoelastic behavior, storage modulus and glass transition of these functionalized nanocomposites.
6. Finally, there is also a need to overcome the problems associated with melt processing such as maintaining lower CNT loadings due to high viscosities of the composites at higher loading of nanotubes.

APPENDIX A: Stress-Strain curve for nanocomposites

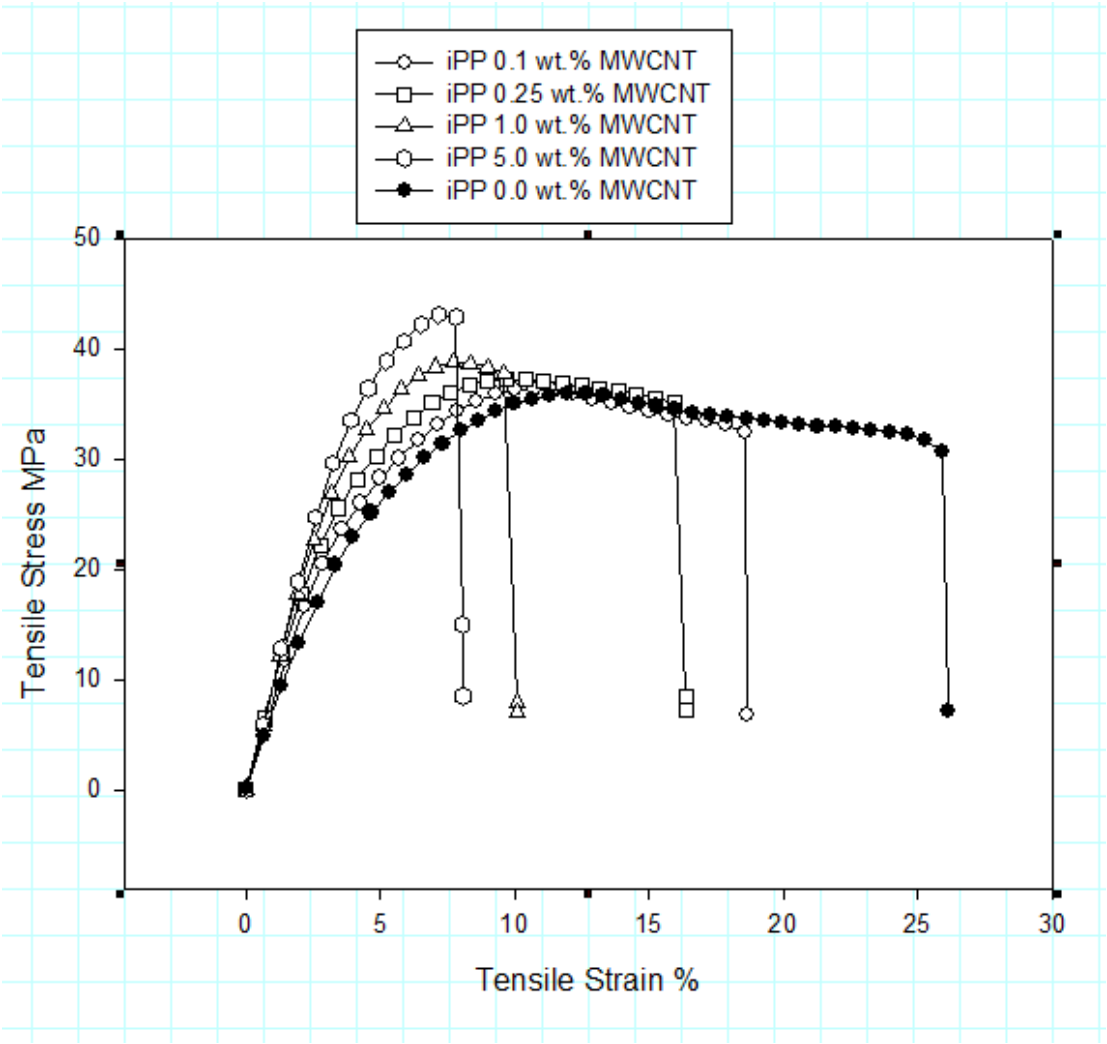

Figure 24: Stress-strain Curves for iPP/MWCNT nanocomposites at 0, 0.1, 0.25, 1.0 & 5.0 wt.% loadings of MWCNT

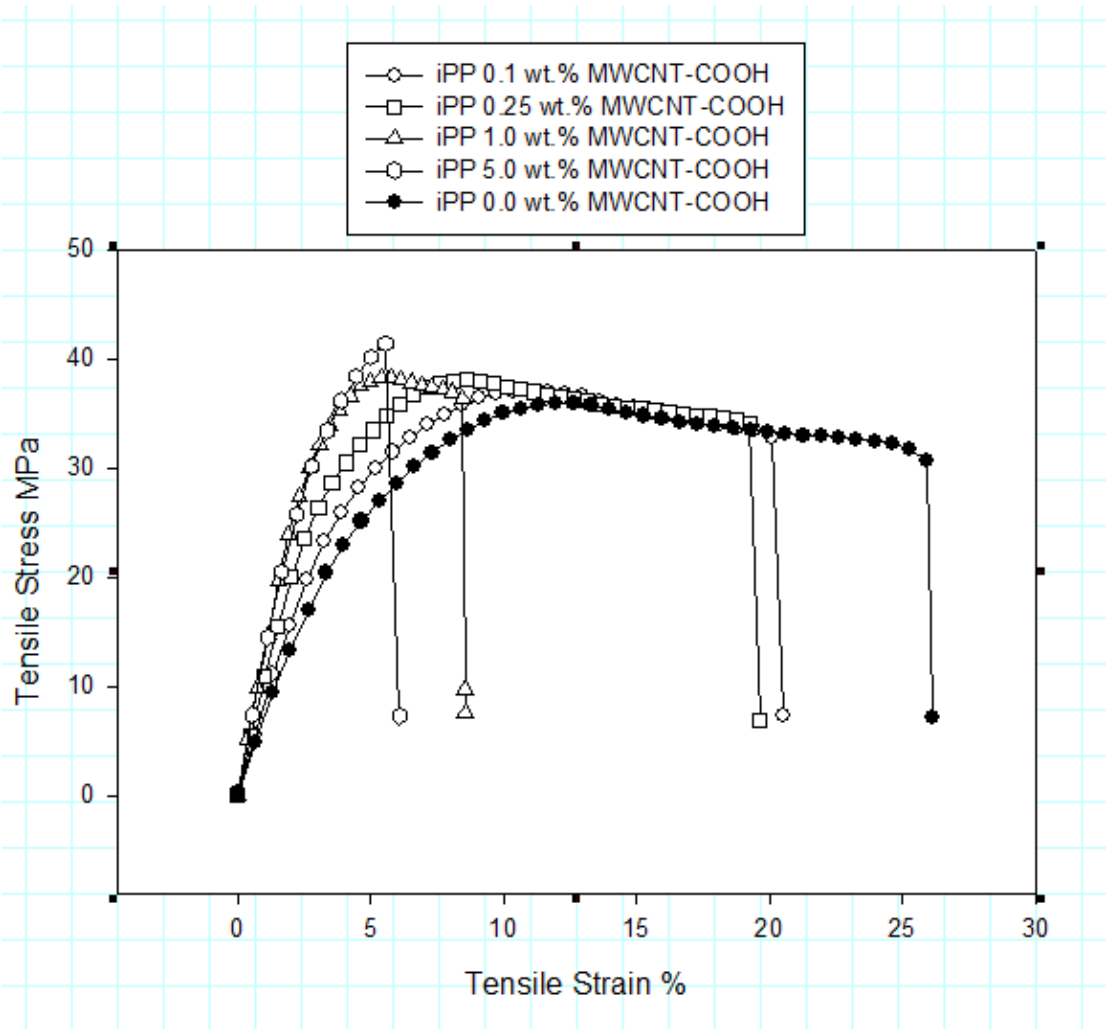

Figure 25: Stress-strain Curves for iPP/MWCNT-COOH nanocomposites at 0, 0.1, 0.25, 1.0 & 5.0 wt.% loadings of MWCNT-COOH

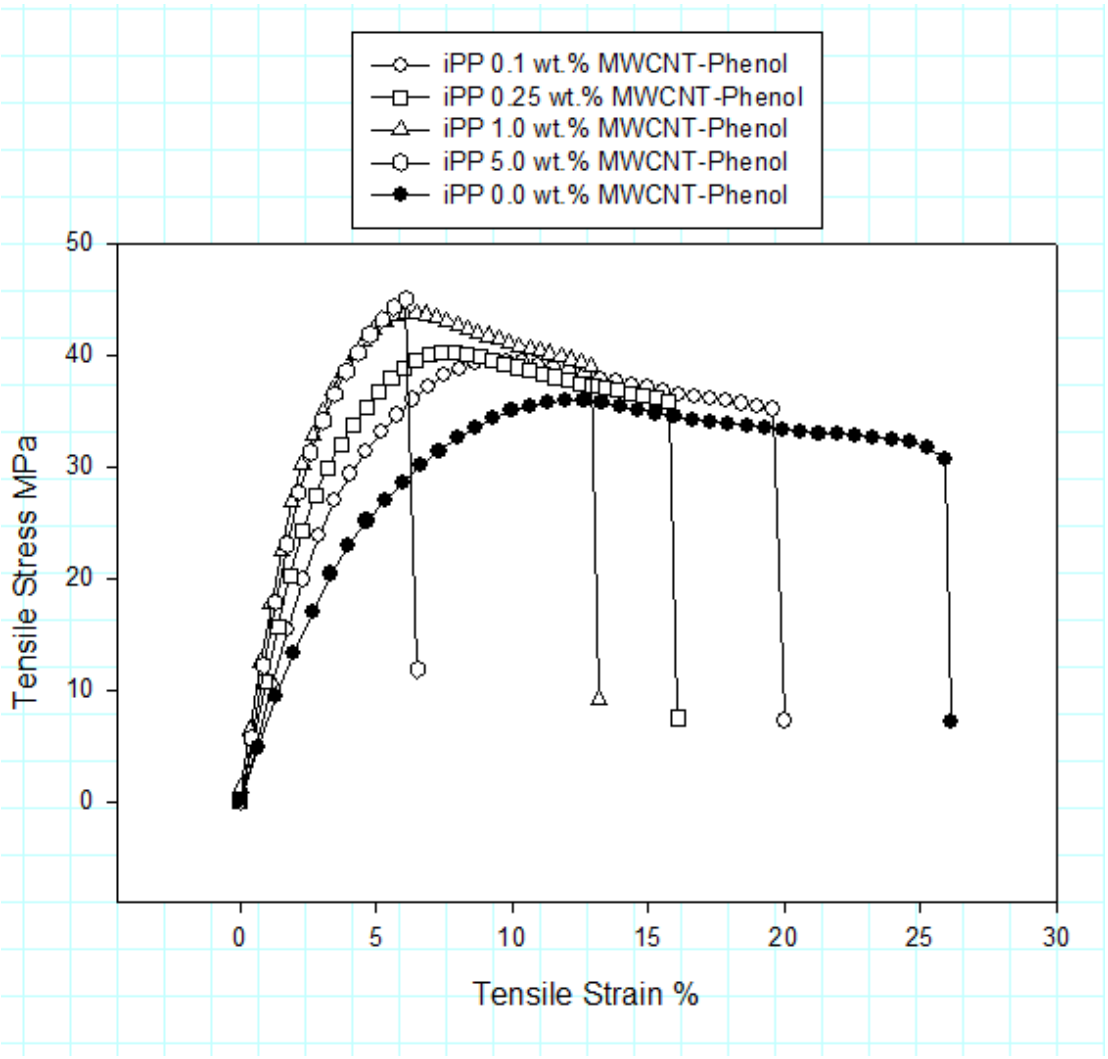

Figure 26: Stress-strain Curves for iPP/MWCNT-Phenol nanocomposites at 0, 0.1, 0.25, 1.0 & 5.0 wt.% loadings of MWCNT-Phenol

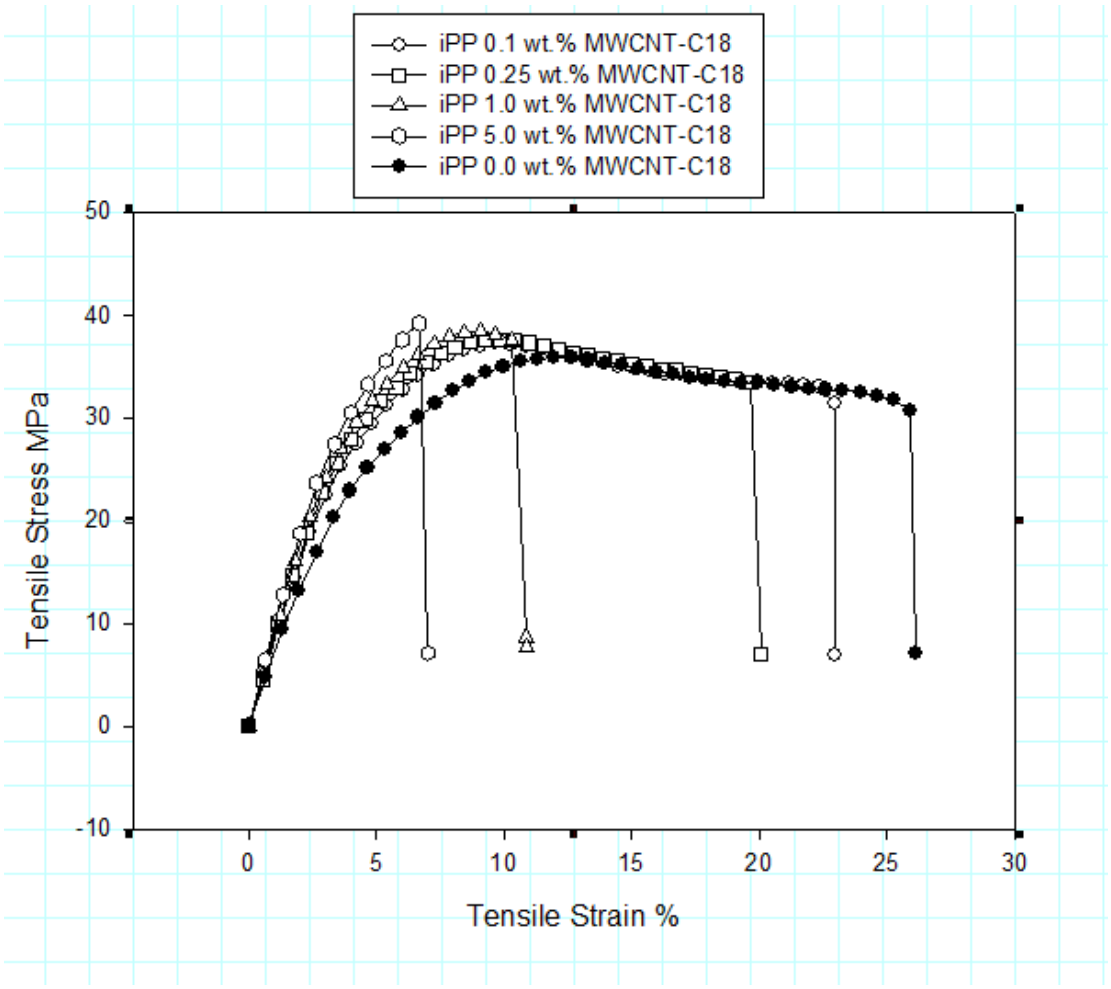

Figure 27: Stress-strain Curves for iPP/MWCNT-C18 nanocomposites at 0, 0.1, 0.25, 1.0 & 5.0 wt.% loadings of MWCNT-C18

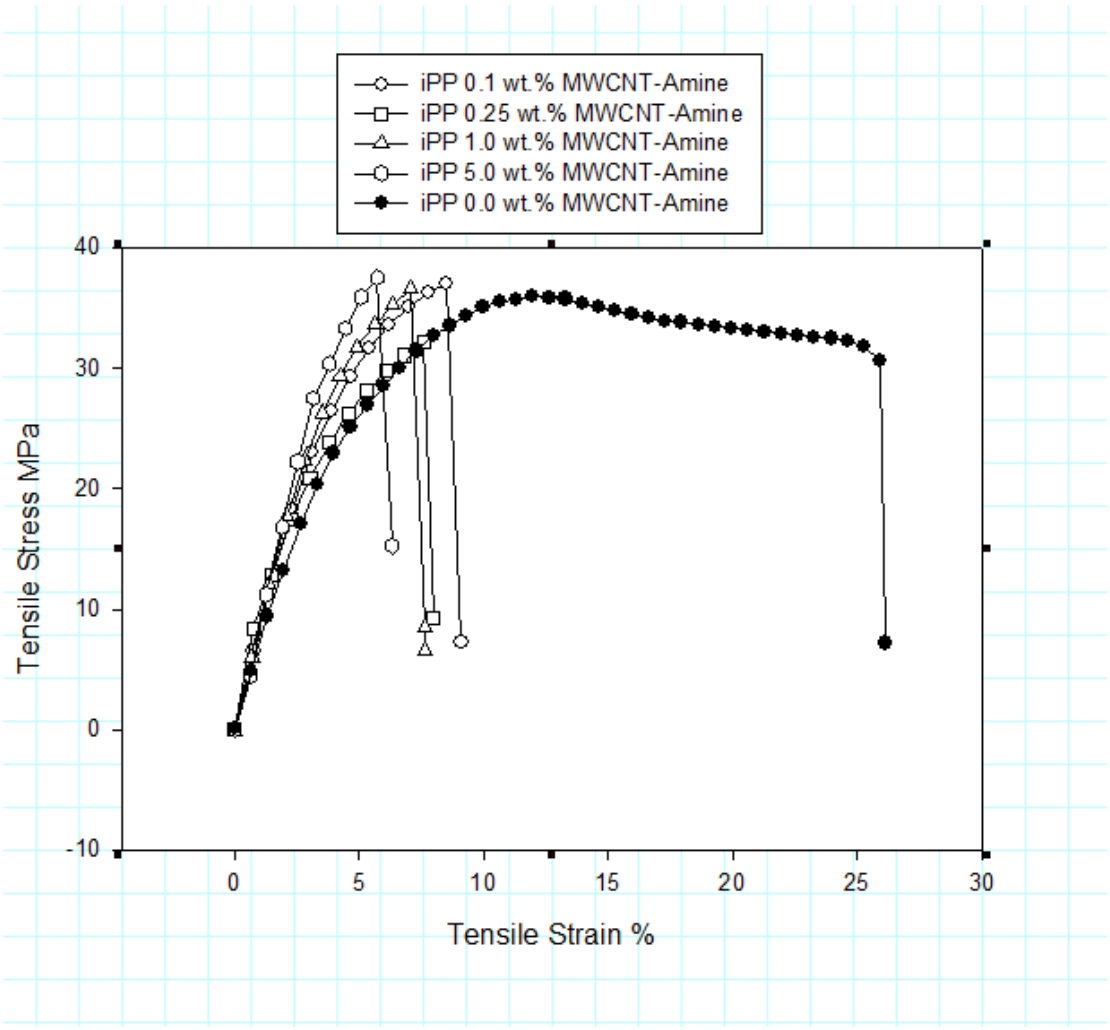

Figure 28: Stress-strain Curves for iPP/MWCNT-Amine nanocomposites at 0, 0.1, 0.25, 1.0 & 5.0 wt.% loadings of MWCNT-Amine

APPENDIX B: Young's Modulus of iPP and iPP/MWCNT nanocomposites Stress-Strain Curve

Appendix B1: Young's Modulus of iPP Stress-Strain Curve

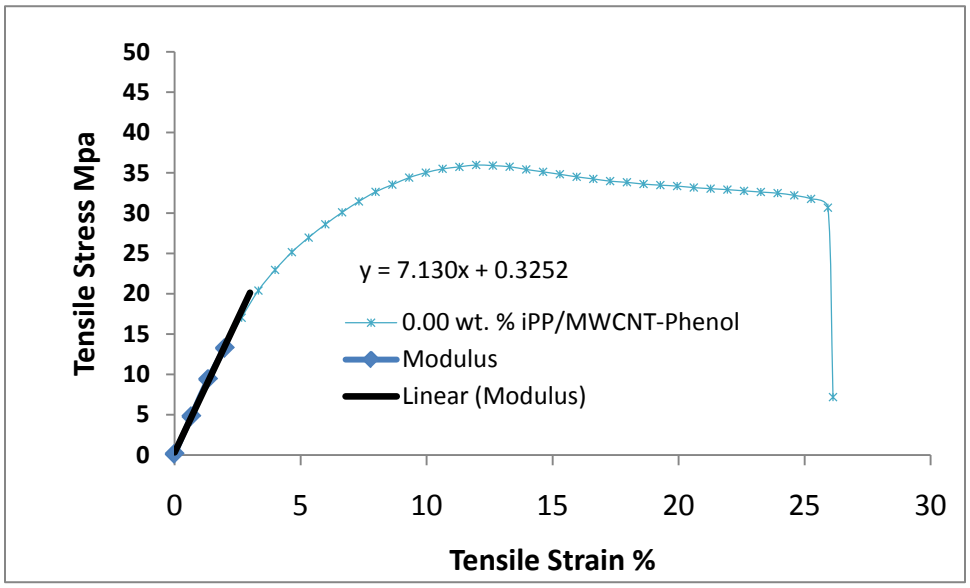

Appendix B2: Young's Modulus of iPP/MWCNT Stress-Strain Curve

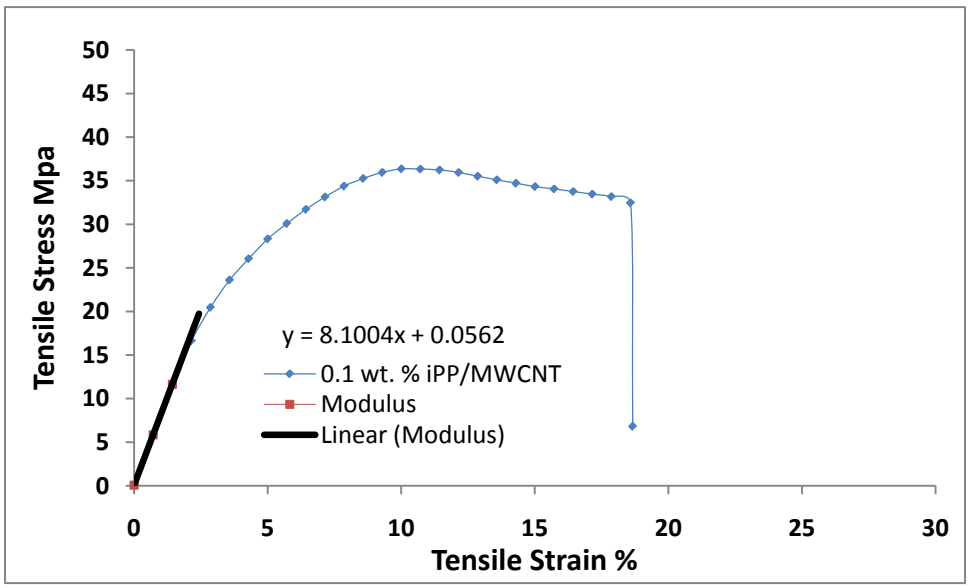

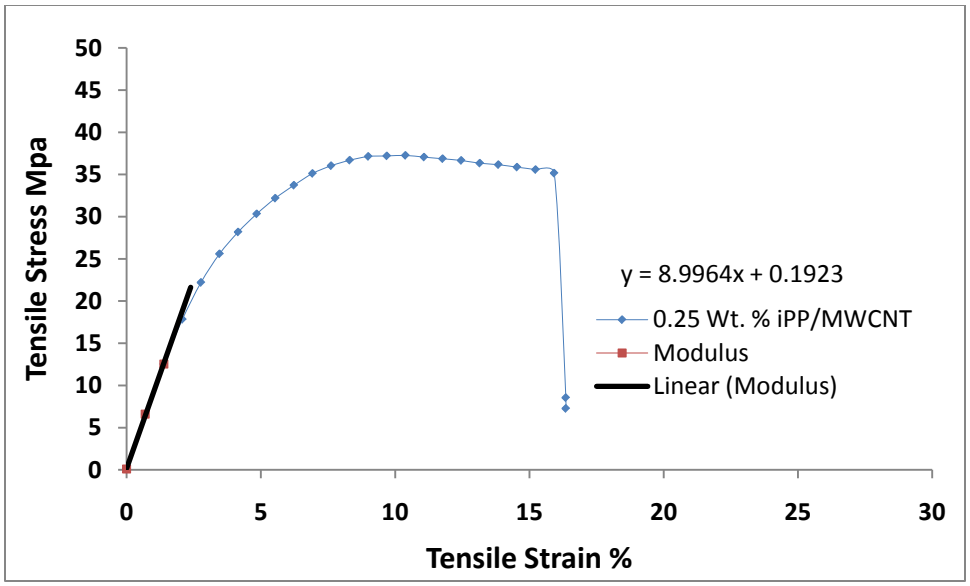
Tensile Stress Mpa
50
45
40
35
30
25
20
15
10
5
0
0
5
10
15
20
25
30
Tensile Strain %
y = 8.9964x + 0.1923
0.25 Wt. % iPP/MWCNT
Modulus
Linear (Modulus)

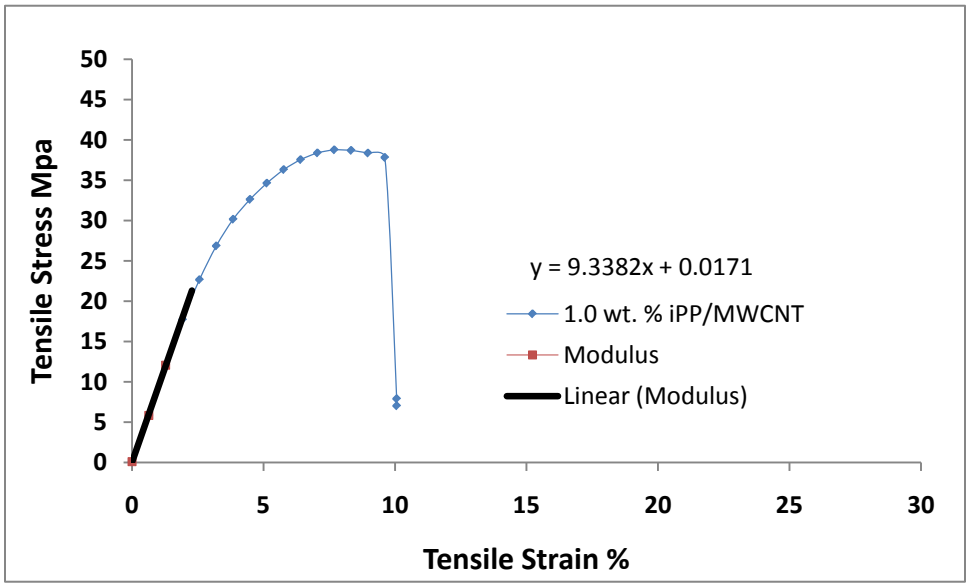
Tensile Stress Mpa
50
45
40
35
30
25
20
15
10
5
0
0
5
10
15
20
25
30
Tensile Strain %
y = 9.3382x + 0.0171
1.0 wt. % iPP/MWCNT
Modulus
Linear (Modulus)

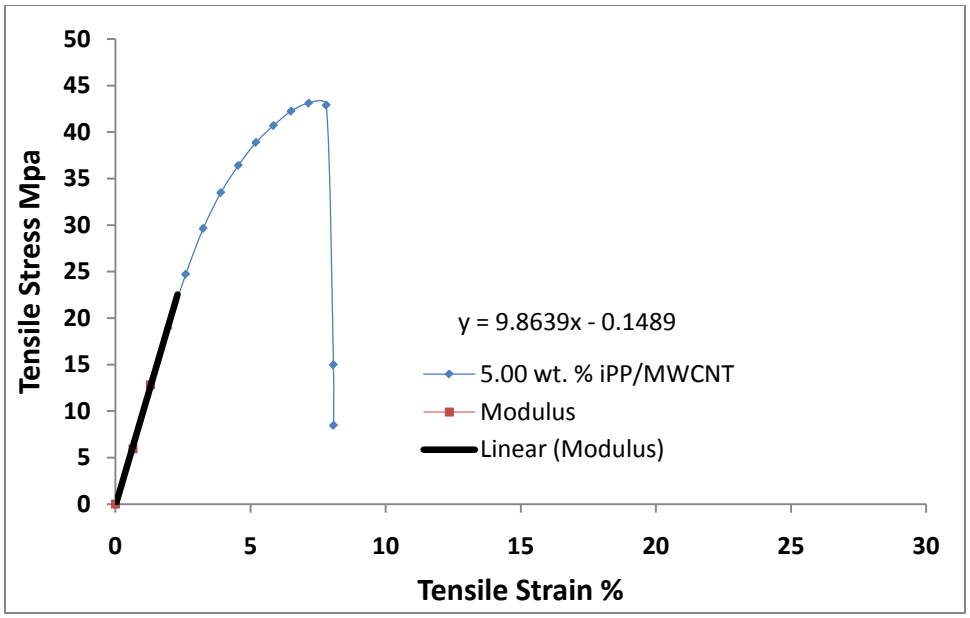

Appendix B3: Young's Modulus of iPP/MWCNT-COOH

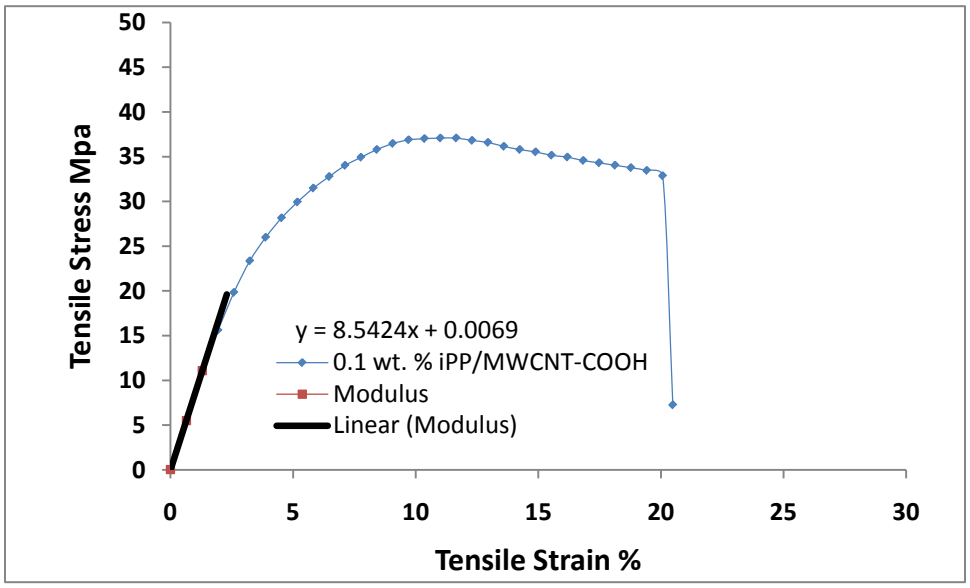

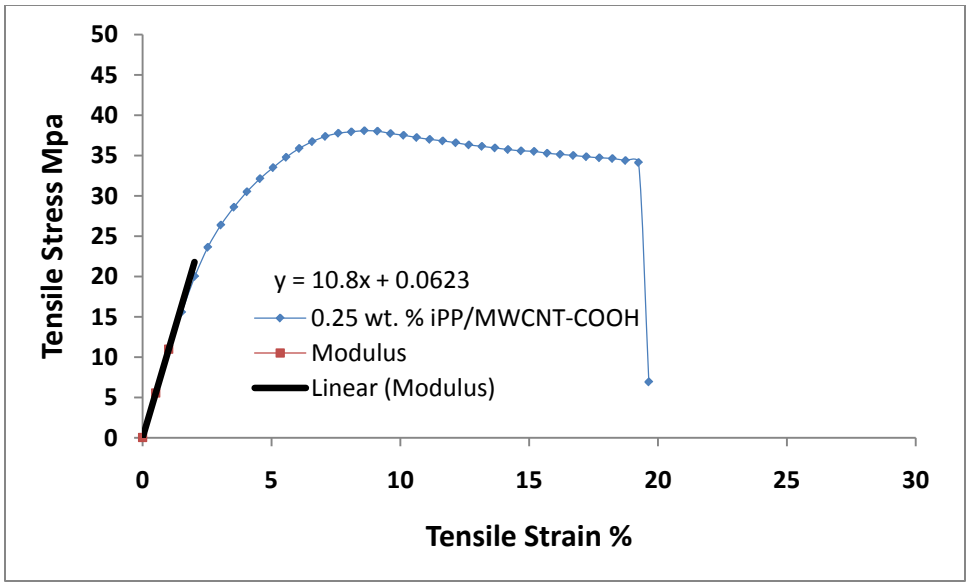
Tensile Stress Mpa
50
45
40
35
30
25
20
15
10
5
0
0
5
10
15
20
25
30
Tensile Strain %
y = 10.8x + 0.0623
0.25 wt. % iPP/MWCNT-COOH
Modulus
Linear (Modulus)

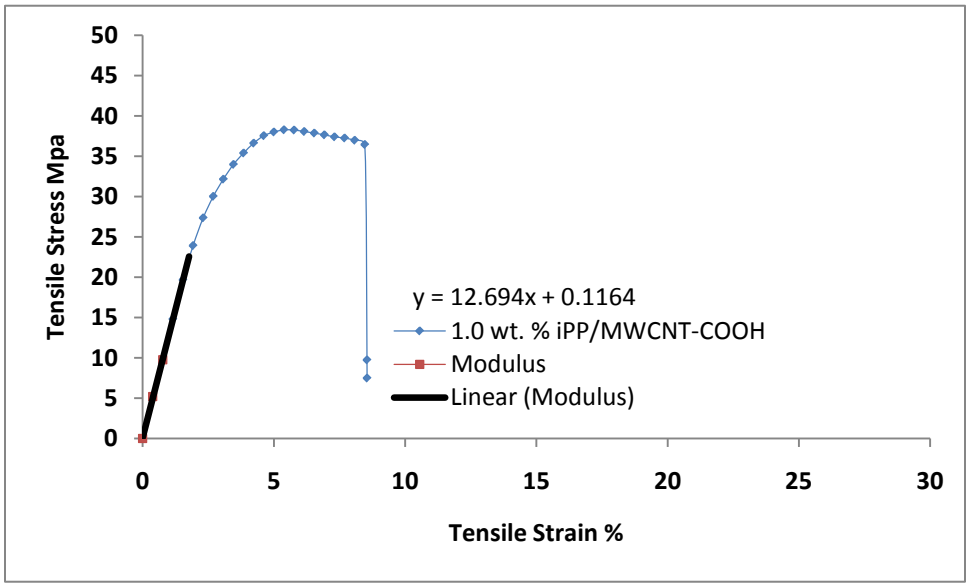
Tensile Stress Mpa
50
45
40
35
30
25
20
15
10
5
0
0
5
10
15
20
25
30
Tensile Strain %
y = 12.694x + 0.1164
1.0 wt. % iPP/MWCNT-COOH
Modulus
Linear (Modulus)

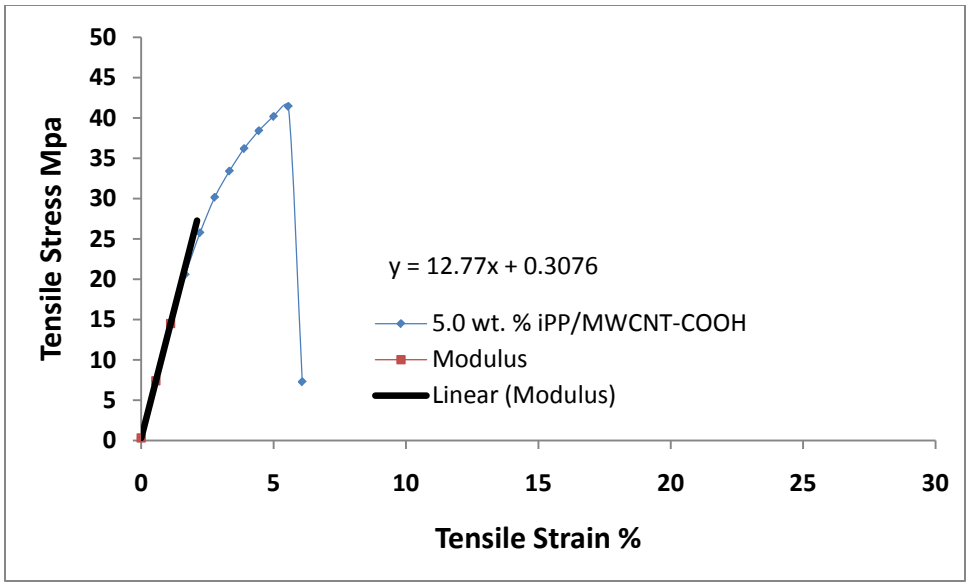

Appendix B4: Young's Modulus of iPP/MWCNT-Phenol

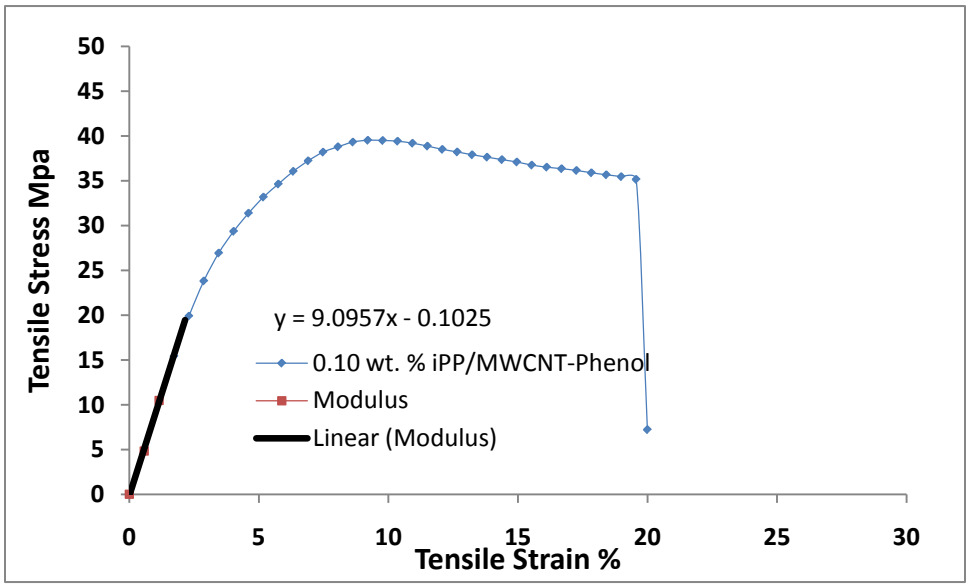

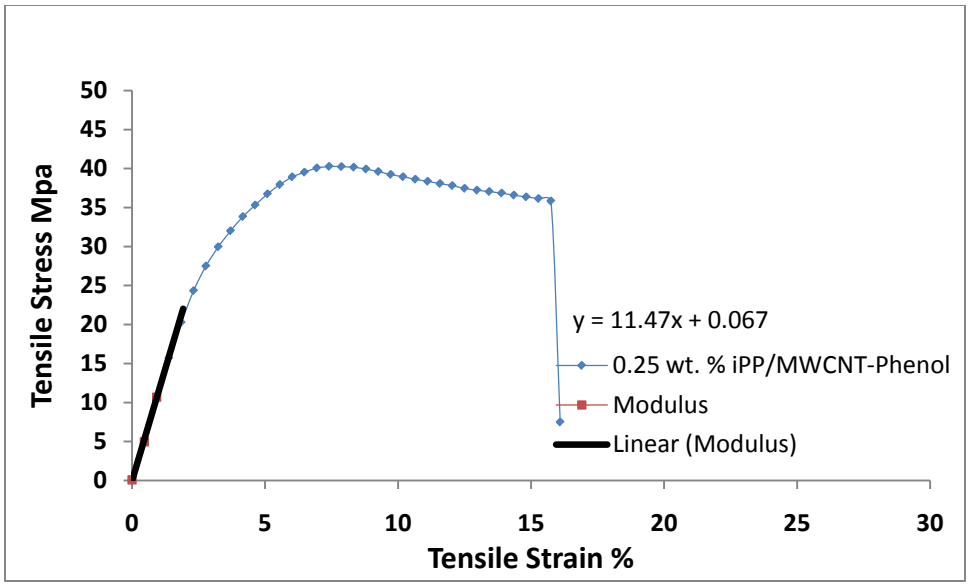
Tensile Stress Mpa
50
45
40
35
30
25
20
15
10
5
0
0
5
10
15
20
25
30
Tensile Strain %
y = 11.47x + 0.067
0.25 wt. % iPP/MWCNT-Phenol
Modulus
Linear (Modulus)

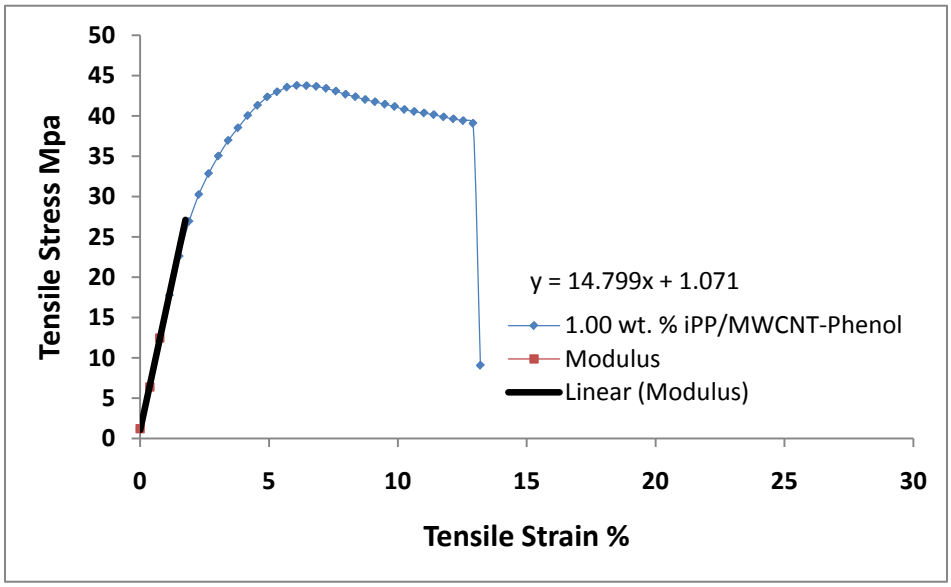
Tensile Stress Mpa
50
45
40
35
30
25
20
15
10
5
0
0
5
10
15
20
25
30
Tensile Strain %
y = 14.799x + 1.071
1.00 wt. % iPP/MWCNT-Phenol
Modulus
Linear (Modulus)

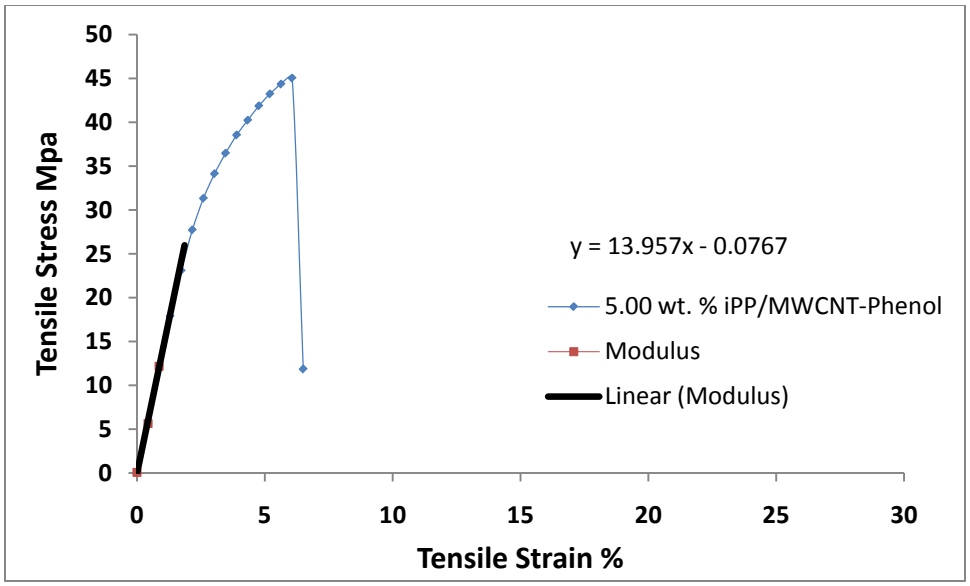

Appendix B5: Young's Modulus of iPP/MWCNT-C18

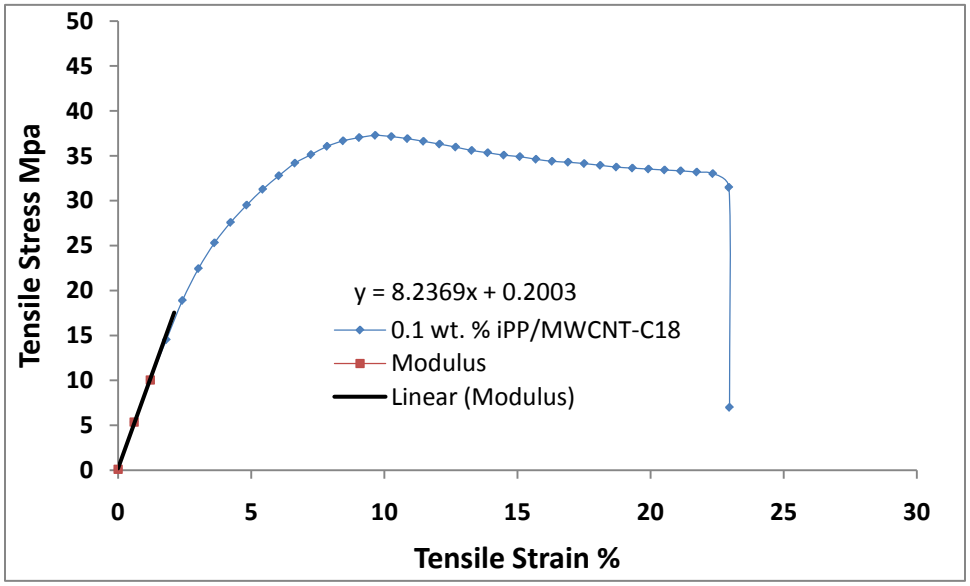

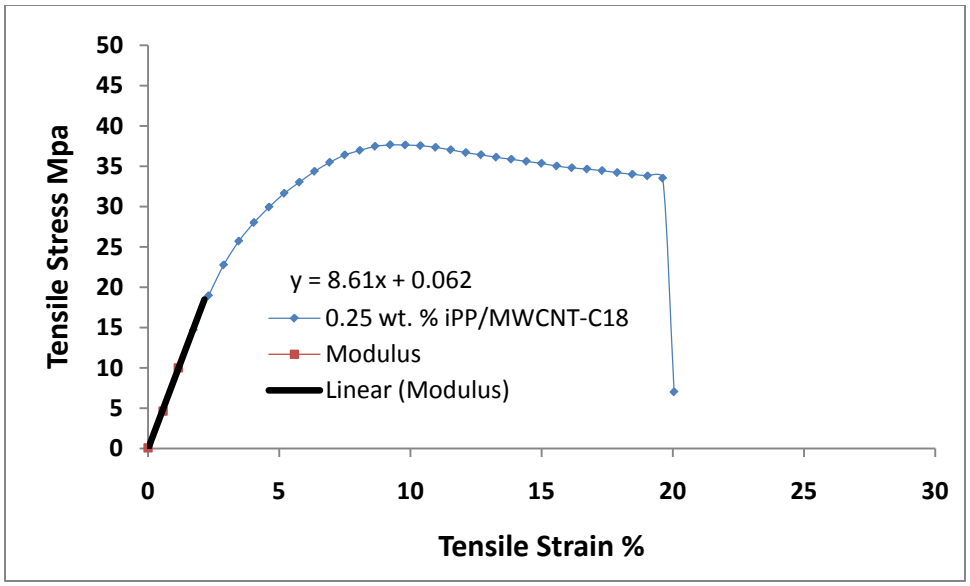
Tensile Stress Mpa
50
45
40
35
30
25
20
15
10
5
0
0
5
10
15
20
25
30
Tensile Strain %
y = 8.61x + 0.062
0.25 wt. % iPP/MWCNT-C18
Modulus
Linear (Modulus)

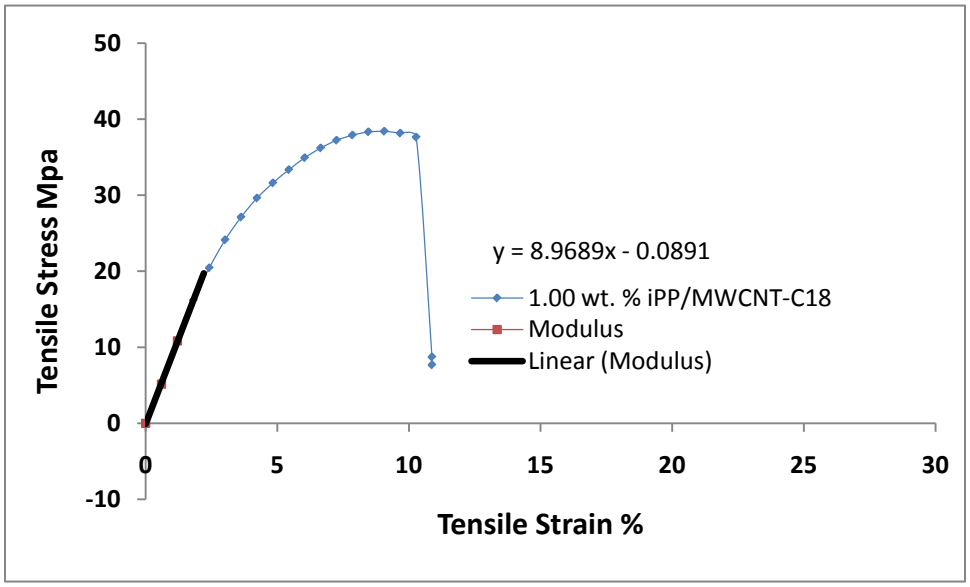
Tensile Stress Mpa
50
40
30
20
10
0
-10
0
5
10
15
20
25
30
Tensile Strain %
y = 8.9689x - 0.0891
1.00 wt. % iPP/MWCNT-C18
Modulus
Linear (Modulus)

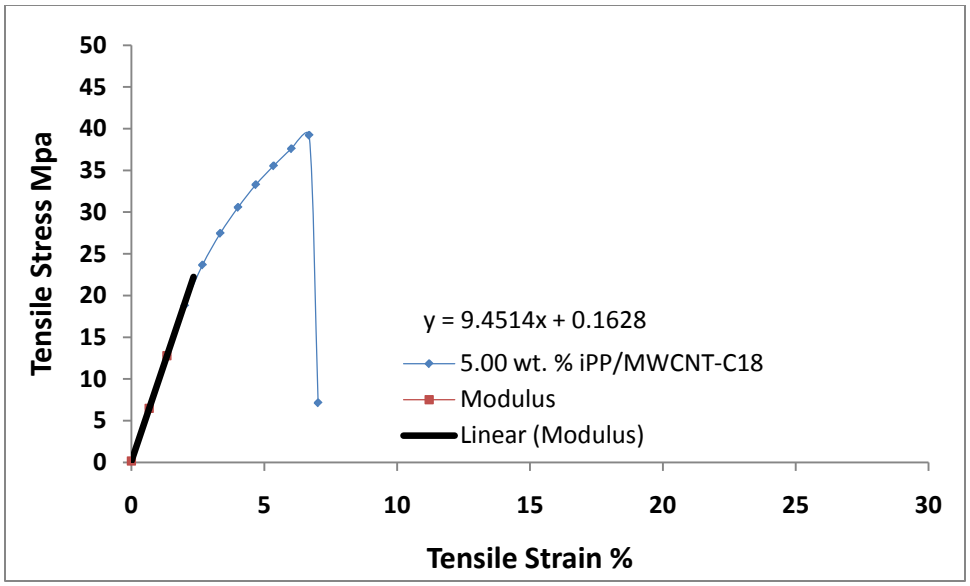

Appendix B6: Young's Modulus of iPP/MWCN-amine

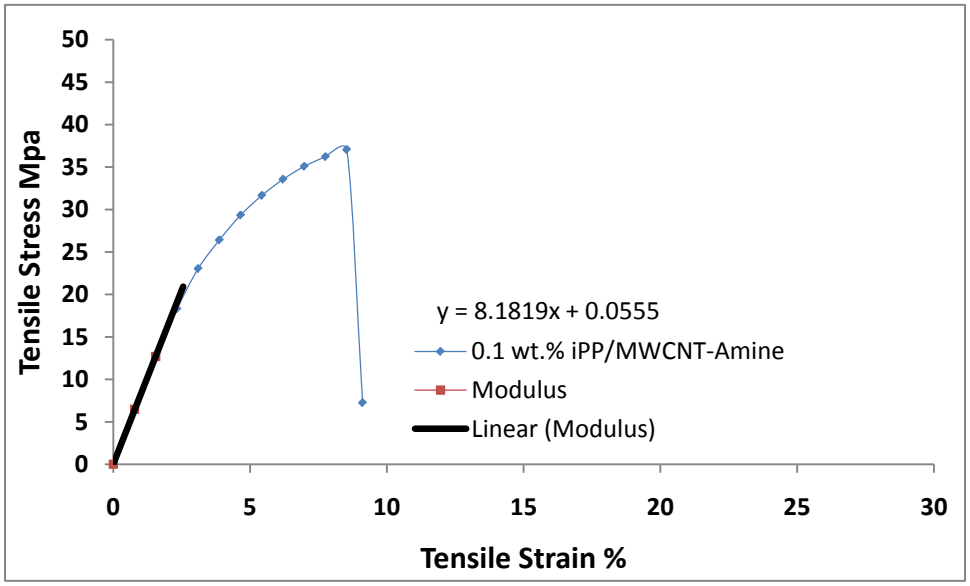

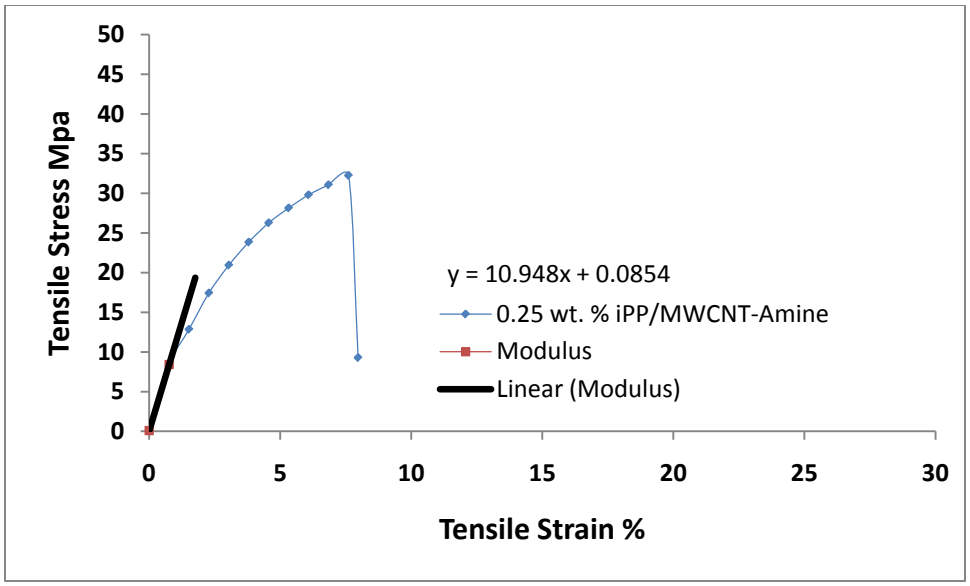
Tensile Stress Mpa
50
45
40
35
30
25
20
15
10
5
0
0
5
10
15
20
25
30
Tensile Strain %
y = 10.948x + 0.0854
0.25 wt. % iPP/MWCNT-Amine
Modulus
Linear (Modulus)

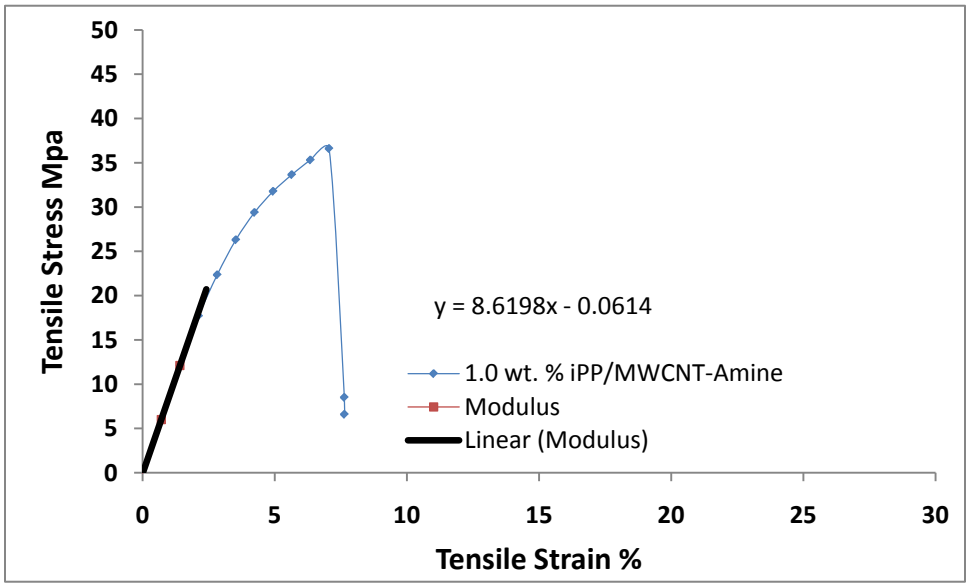
Tensile Stress Mpa
50
45
40
35
30
25
20
15
10
5
0
0
5
10
15
20
25
30
Tensile Strain %
y = 8.6198x - 0.0614
1.0 wt. % iPP/MWCNT-Amine
Modulus
Linear (Modulus)

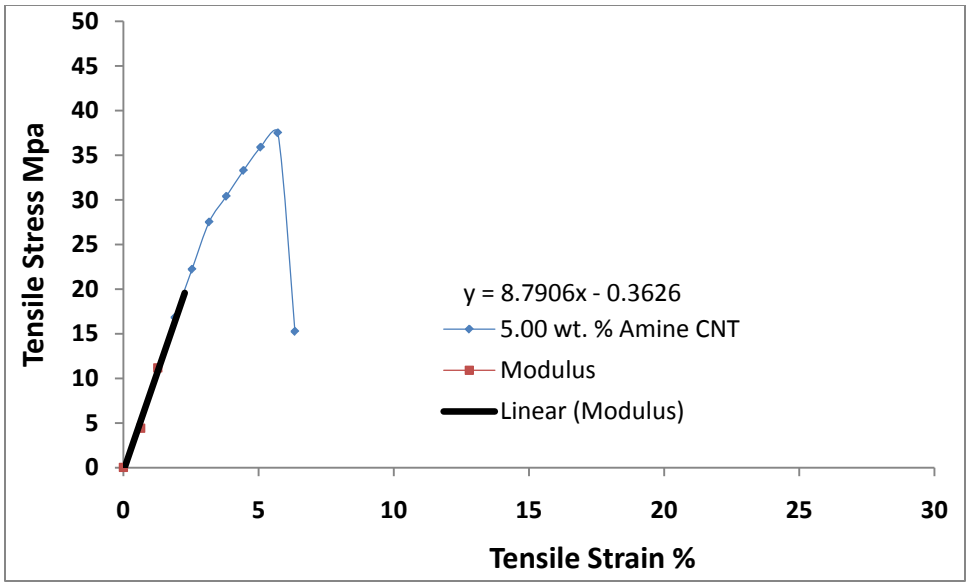
Tensile Stress Mpa
50
45
40
35
30
25
20
15
10
5
0
0
5
10
15
20
25
30
Tensile Strain %
y = 8.7906x - 0.3626
5.00 wt. % Amine CNT
Modulus
Linear (Modulus)

APPENDIX C: Nomenclatures

aPP	atactic polypropylene
CNTs	Carbon nanotubes
DIPM	Dynamic packing injection molding
DMA	Dynamic mechanical analysis
DSC	Differential scanning spectrometer
FTIR	Fourier Transform Infrared Spectroscopy
iPP	Isotactic polpropylene
MFS	Melt fiber spinning
MWCNT	Multiwall carbon nanotube
PMMA	Poly methyl methacrylate
PMMM	Pan milling melt mixing
PP	Polypropylene
SEM	Scanning electron microscopy
SMFS	Solution mixing fiber spinning
SMMS	Solvent mixing melt spinning
SMS	Solution mixing spinning
SWCNT	Single wall carbon nanotube
XRD	X-ray diffraction

REFERENCES

1. Ajayan PM, Stephan O, Colliex C, Trauth D., Science 1994, 265, 1212–1214
2. Andrews R, Wisenberger M. C., Carbon Solid State Mater Sci, 2004, 8, 31–37.
3. Assouline, E.; Lustiger, A.; Barber, A. H.; Cooper, C. A.; Klein, E.; Wachtel, E.; Wagner, H. D. J Polym Sci Part B: Polym Phys 2003, 41, 520–527.
4. Bhattacharyya, A. R.; Sreekumar, T. V.; Liu, T.; Kumar, S.; Ericson, L. M.; Hauge, R. H.; Smalley, R. E. Polymer 2003, 44, 2373–2377.
5. Bin, Y. Z.; Kitanaka, M.; Zhu, D.; Matsuo, M. Macromolecules 2003, 36, 6213–6219.
6. Bubert, H.; Haiber, S.; Brandl, W.; Marginean, G.; Heintze, M.; Bruser, V. Diam Relat Mater 2003, 12, 811–815.
7. Chang TE, Jensen LR, Kisliuk A, Pipes RB, Pyrz R, Sokolov AP., Polymer 2005;46:439–444.
8. Chen, G. Z.; Shaffer, M. S. P.; Coleby, D.; Dixon, G.; Zhou, W.; Fray, D. J.; Windle, A. H. Adv Mater 2000, 12, 522–526.
9. Chen, J.; Hamon, M. A.; Hu, H.; Chen, Y.; Rao, A. M.; Eklund, P. C.; Haddon, R. C. Science 1998, 282, 95–98.
10. Deng, J.; Ding, X.; Zhang, W.; Peng, Y.; Wang, J.; Long, X.; Li, P.; Chan, A. S. C. Eur Polym J 2002, 38, 2497–2501.
11. Dondero W E, R E Gorga, J. Polymer Sci. B, 2006, 44, 864-878.

12. Dror, Y.; Salalha, W.; Khalfin, R. L.; Cohen, Y.; Yarin, A. L.; Zussman, E. Langmuir 2003, 19, 7012–7020.
13. Ebbesen, T. W.; Lezec, H. J.; Hiura, H.; Bennett, J. W.; Ghaemi, H. F.; Thio, T. Nature 1996, 382, 54–56.
14. Gong, X.; Liu, J.; Baskaran, S.; Voise, R. D.; Young, J. S. Chem Mater 2000, 12, 1049–1052.
15. Gorga, R. E.; Cohen, R. E. J Polym Sci Part B: Polym Phys 2004, 42, 2690–2702.
16. Grady, B. P.; Pompeo, F.; Shambaugh, R. L. Resasco, D. E. J Phys Chem B 2002, 106, 5852- 5858.
17. Iijima, S., T. Nature 1999, 354, 56.
18. Jang, J.; Bae, J.; Yoon, S. H. J Mater Chem 2003, 13, 676-681.
19. Jia, Z.; Wang, Z.; Xu, C.; Liang, J.; We, B.; Wu, D.; Zhu, S. Mater Sci Eng A 1999, 271, 395–400.
20. Jin, Z.; Pramoda, K. P.; Xu, G.; Goh, S. H. Chem. Phys Lett 2001, 337, 43–47.
21. Kashiwagi T, Grulke E, Hilding J, Groth K, Harris R, Butler K, cShields J, Kharchenko S, Douglas J, Polymer, 2004, 45, 4227-4239.
22. Kearns, J. C.; Shambaugh, R. L. J Appl Polym Sci 2002, 86 2079–2084.
23. Leelapornpisit W., Ton-That M-T, Perrin-Sarazin F, Cole K C, Denault J, Simard B, J. Polymer Sci B, 2005, 43, 2445-2453.
24. Manchado M A, Valentini L, Biagiotti J, Kenny J M, Carbon, 2005 43, 1499-1505.

25. McIntosh, Khabashesku VN, Barrera EV., Chem Mater 2006;18:4561–9.
26. Mitan, A.; Jiang, K.; Dukes, D.; Andrews, R.; Schadler, L. S. Chem Mater 2003, 15, 3198–3201.
27. Mitchell, C. A.; Bahr, J. L.; Arepalli, S.; Tour, J. M.; Krishnamoorti, R. Macromolecules 2002 35, 8825–8830.
28. Moore, E. M.; Ortiz, D. L.; Marla, V. T.; Shambaugh, R. L.; Grady, B. P. J Appl Polym Sci 2004, 93, 2926–2933.
29. Potschke P., Bhattacharyya A., Janke A., Goering H., Compos Interfaces, 2003 10, 389–404.
30. Potschke, P.; Bhattacharyya, A. R.; Janke, A. Eur Polym J 2004, 40, 137–148.
31. Qian, D.; Dickey, E. C.; Andrews, R.; Rantell, T. Appl Phys Lett 2000, 76, 2868–2870.
32. Ruoff S. R. and Lorents C. D., Carbon 1995, 33, 925.
33. Safadi, B.; Andrews, R.; Grulke, E. A. J Appl Polym Sci 2002, 84, 2660–2669.
34. Sandler, J.; Broza, G.; Nolte, M.; Schulte, K.; Lam, Y. M.; Shaffer, M. S. P. J Macromol Sci Phys 2003, B42, 479–488.
35. Seo M-K, Lee J-R, Park S-J, Materials Sci. Eng. A 2005, 404, 79-84.
36. Seo M-K, Park S-J, Chemical Physics Letters, 2004, 395, 44-48.
37. Shaffer, M. S. P.; Fan, X.; Windle, A. H. Carbon 1998, 36, 1603–1612.
38. Siochi, E. J.; Working, D. C.; Park, C.; Lillehei, P. T.; Rouse, J. H.; Topping, C. C.; Bhattacharyya, A. R.; Kumar, S. Compos B 2004, 35, 439–446.

39. Socrates G., Infrared Characteristic Group and Frequencies, John Wiley & Sons, New York, 1980

40. Star, A.; Stoddart, J. F.; Steuerman, D.; Diehl, M.; Boukai, A.; Wong, E. W.; Yang, X.; Chung, S.-W.; Choi, H.; Heath, J. R. Angew Chem Int Ed 2001, 40, 1721–1725.

41. Tang, W. Z.; Santare, M. H.; Advani, S. G. Carbon 2003, 41, 2779–2785.

42. Treacy M. M. J., Ebbesen T. W., Gibson J. M., Nature, 1996, 381, 678.

43. Valentini, L.; Biagiotti, J.; Kenny, J. M.; Santucci, S. Compos Sci Technol 2003, 63, 1149–1153.

44. Valentini, L.; Biagiotti, J.; Kenny, J. M.; Santucci, S. J Appl Polym Sci 2003, 87, 708–713.

45. Wong W, E. and Sheehan E. P., Science, 1997, 277, 1971

46. Xia H, Wang Q, Li K, Hu GH., J Appl Polym Sci 2004;93:378–86.

47. Xia, H. S.; Wang, Q.; Li, K. S.; Hu, G. H. J Appl Polym Sci 2004, 93, 378–386.

48. Xiao Y, Zhang X, Cao W, Wang K, Tan H, Zhang Q, et al., J Appl Polym Sci 2007;104:1880–6.

49. Yang J, Lin Y, Wang J, Lai M, Li J, Liu J, Tong X, Cheng H, J. Applied Polymer Sci., 2005, 98, 1087-1091.

50. Zdenko S., Tasis D., Papagelis K., Costas G., Prog in Polym Sci., 2008, doi:10.1016/j.progpolymsci.2009.09.03

51. Zhao P, Wang K, Yang H, Zhang Q, Du R, Fu G., Polymer 2007;48:5688–95.

52. Yamabe, T., Recent Development in Carbon Nanotubes Synthesis Met (19950, pp. 1511-1518

VITAE

NAME:	Salihu Adamu Girei
NATIONALITY:	Nigerian
DATE OF BIRTH:	June 6, 1978
PLACE OF BIRTH:	Jimeta-Yola
EMAIL:	asgirei@yahoo.com
MOBILE:	+966530042858

EDUCATION:

B.Eng (HONS) Chemical Engineering

Federal University of Technology Yola,

Adamawa State, Nigeria

2005

MSc Chemical Engineering

King Fahd University of Petroleum & Minerals,

Dhahran, Kingdom of Saudi Arabia

2010